EUROPEAN ORGANIZATION FOR NUCLEAR RESEARCH (CERN)
FERMILAB-PUB-11-767-CMS

CERN-PH-EP/2010-094
2011/05/30

CMS-QCD-10-007

# Strange Particle Production in pp Collisions at $\sqrt{s}$ = 0.9 and 7 TeV

The CMS Collaboration*

arXiv:1102.4282v2 [hep-ex] 27 May 2011

## Abstract

The spectra of strange hadrons are measured in proton-proton collisions, recorded by the CMS experiment at the CERN LHC, at centre-of-mass energies of 0.9 and 7 TeV. The $K^0_S$, $\Lambda$, and $\Xi^-$ particles and their antiparticles are reconstructed from their decay topologies and the production rates are measured as functions of rapidity and transverse momentum, $p_T$. The results are compared to other experiments and to predictions of the PYTHIA Monte Carlo program. The $p_T$ distributions are found to differ substantially from the PYTHIA results and the production rates exceed the predictions by up to a factor of three.

*Submitted to the Journal of High Energy Physics*

*See Appendix A for the list of collaboration members

Operated by Fermi Research Alliance, LLC under Contract No. De-AC02-07CH11359 with the United States Department of Energy.

# 1 Introduction

Measurements of particle yields and spectra are an essential step in understanding proton-proton collisions at the Large Hadron Collider (LHC). The Compact Muon Solenoid (CMS) Collaboration has published results on spectra of charged particles at centre-of-mass energies of 0.9, 2.36, and 7 TeV [1, 2]. In this analysis the measurement is extended to strange mesons and baryons ($K^0_S$, $\Lambda$, $\Xi^-$) [1] at centre-of-mass energies of 0.9 and 7 TeV. The investigation of strange hadron production is an important ingredient in understanding the nature of the strong force. The LHC experiments ALICE and LHCb have recently reported results on strange hadron production at $\sqrt{s} = 0.9$ TeV [3, 4]. In addition to results at $\sqrt{s} = 0.9$ TeV, we also present results at $\sqrt{s} = 7$ TeV, opening up a new energy regime in which to study the strong interaction. As the strange quark is heavier than up and down quarks, production of strange hadrons is generally suppressed relative to hadrons containing only up and down quarks. The amount of strangeness suppression is an important component in Monte Carlo (MC) models such as PYTHIA [5] and HIJING/B$\bar{\text{B}}$ [6]. Because the threshold for strange quark production in a quark-gluon plasma is much smaller than in a hadron gas, an enhancement in strange particle production has frequently been suggested as an indication of quark-gluon plasma formation [7]. This effect would be further enhanced in baryons with multiple strange quarks. While a quark-gluon plasma is more likely to be found in collisions of heavy nuclei, the enhancement of strange quark production in high energy pp collisions would be a sign of a collective effect, according to some models [8, 9]. In contrast, recent Regge-theory calculations indicate little change in the ratio of $K^0_S$ to charge particle production with increasing collision energy [10, 11]. Thus, these measurements can be used to constrain theories, provide input for tuning of Monte Carlo models, and serve as a reference for the interpretation of strangeness production results in heavy-ion collisions.

Minimum bias collisions at the LHC can be classified as elastic scattering, inelastic single-diffractive dissociation (SD), inelastic double-diffractive dissociation, and inelastic non-diffractive scattering. The results presented here are normalized to the sum of double-diffractive and non-diffractive interactions, referred to as non-single-diffractive (NSD) interactions [1, 2]. This choice is made to most closely match the event selection and to compare with previous experiments, which often used similar criteria. The $K^0_S$, $\Lambda$, and $\Xi^-$ are long-lived particles ($c\tau > 1$ cm) and can be identified from their decay products originating from a displaced vertex. The particles are reconstructed from their decays: $K^0_S \to \pi^+\pi^-$, $\Lambda \to p\pi^-$, and $\Xi^- \to \Lambda\pi^-$ over the rapidity range $|y| < 2$, where the rapidity is defined as $y = \frac{1}{2}\ln\frac{E+p_L}{E-p_L}$, $E$ is the particle energy, and $p_L$ is the particle momentum along the anticlockwise beam direction. For each particle species, we measure the production rate versus rapidity and transverse momentum $p_T$, the average $p_T$, the central production rate $\frac{dN}{dy}|_{y\approx 0}$, and the integrated yield for $|y| < 2$ per NSD event. We compare our measurements to results from Monte Carlo models and lower energy data.

# 2 CMS experiment and collected data

CMS is a general purpose experiment at the LHC [12]. The silicon tracker, lead-tungstate crystal electromagnetic calorimeter, and brass-scintillator hadron calorimeter are all immersed in a 3.8 T axial magnetic field while muon detectors are interspersed with flux return steel outside of the 6 m diameter superconducting solenoid. The silicon tracker is used to reconstruct charged particle trajectories with $|\eta| < 2.5$, where the pseudorapidity is defined as $\eta = -\ln\tan\frac{\theta}{2}$, $\theta$

[1] Particle-conjugate states are implied throughout this paper.

being the polar angle with respect to the anticlockwise beam. The tracker consists of layers of $100 \times 150$ $\mu m^2$ pixel sensors at radii less than 15 cm and layers of strip sensors, with pitch ranging from 80 to 183 $\mu$m, covering radii from 25 to 110 cm. In addition to barrel and endcap detectors, CMS has extensive forward calorimetry including a steel and quartz-fibre hadron calorimeter (HF), which covers $2.9 < |\eta| < 5.2$. The data presented in this paper were collected by the CMS experiment in spring 2010 from proton-proton collisions at centre-of-mass energies of 0.9 and 7 TeV during a period in which the probability for two collisions in the same bunch crossing was negligible and the bunch crossings were well separated.

The online selection of events required activity in the beam scintillator counters at $3.23 < |\eta| < 4.65$ in coincidence with colliding proton bunches. The offline selection required deposits of at least 3 GeV of energy in each end of the HF [1], preferentially selecting NSD events. A primary vertex reconstructed in the tracker was required and beam-halo and other beam-related background events were rejected as described in Ref. [1]. The data selected with these criteria contain 9.08 and 23.86 million events at 0.9 and 7 TeV, corresponding to approximate integrated luminosities of 240 and 480 $\mu b^{-1}$, respectively. To determine the acceptance and efficiency, minimum-bias Monte Carlo samples were generated at both centre-of-mass energies using PYTHIA 6.422 [5] with tune D6T [13]. These events were passed through a CMS detector simulation package based on GEANT 4 [14].

## 3 Strange particle reconstruction

Ionization deposits recorded by the silicon tracker are used to reconstruct tracks. To maximize reconstruction efficiency, we use a combined track collection formed from merging tracks found with the standard tracking described in Ref. [15] and the minimum bias tracking described in Ref. [1]. Both tracking collections use the same basic algorithm; the differences are in the requirements for seeding, propagating, and filtering tracks.

As described in Ref. [15], the $K^0_S$ and $\Lambda$ (generically referred to as $V^0$) reconstruction combines pairs of oppositely charged tracks; if the normalized $\chi^2$ of the fit to a common vertex is less than 7, the candidate is kept. The primary vertex is refit for each candidate, removing the two tracks associated with the $V^0$ candidate. The next two paragraphs describe the selection of candidates for measurement of $V^0$ and $\Xi^-$ properties, respectively. Selection variables are measured in units of $\sigma$, the calculated uncertainty including all correlations.

To remove $K^0_S$ particles misidentified as $\Lambda$ particles and vice versa, the $K^0_S(\Lambda)$ candidates must have a corresponding $p\pi^-(\pi^+\pi^-)$ mass more than $2.5\sigma$ away from the world-average $\Lambda(K^0_S)$ mass. The production cross sections we measure are intended to represent the prompt production of $K^0_S$ and $\Lambda$, including strong and electromagnetic decays. However, $V^0$ particles can also be produced from weak decays and from secondary nuclear interactions. These unwanted contributions are reduced by requiring that the $V^0$ momentum vector points back to the primary vertex. This is done by requiring the 3D distance of closest approach of the $V^0$ to the primary vertex to be less than $3\sigma$. To remove generic prompt backgrounds, the 3D $V^0$ vertex separation from the primary vertex must be greater than $5\sigma$ and both $V^0$ daughter tracks must have a 3D distance of closest approach to the primary vertex greater than $3\sigma$. With the above selection, the background level for low transverse-momentum $\Lambda$ candidates remains high. Therefore, additional cuts are applied to $\Lambda$ candidates with $p_T < 0.6\,\mathrm{GeV}/c$:

- 3D separation between the primary and $\Lambda$ vertices $> 10\sigma$ (instead of $> 5\sigma$),
- transverse (2D) separation between the pp collision region (beamspot) and $\Lambda$ vertex $> 10\sigma$ (instead of no cut), where the uncertainty is dominated by the $\Lambda$ vertex, and

- 3D impact parameter of the pion and proton tracks with respect to the primary vertex $> (7 - 2|y|)\sigma$ (instead of $> 3\sigma$) where $y$ is the rapidity of the $\Lambda$ candidate. The rapidity dependence is a consequence of the observation that, for the low transverse momentum candidates, large backgrounds dominate at small rapidity, while low efficiency characterizes the large rapidity behaviour.

The resulting mass distributions of $K^0_S$ and $\Lambda$ candidates from the 0.9 and 7 TeV data are shown in Figs. 1 and 2. The $\pi^+\pi^-$ mass distribution is fit with a double Gaussian (with a common mean) signal function plus a quadratic background. The $p\pi^-$ mass distribution is fit with a double Gaussian (common mean) signal function and a background function of the form $Aq^B$, where $q = M_{p\pi^-} - (m_p + m_{\pi^-})$, $M_{p\pi^-}$ is the $p\pi^-$ invariant mass, and $A$ and $B$ are free parameters. The fitted $K^0_S$ ($\Lambda$) yields at $\sqrt{s} = 0.9$ and 7 TeV are $1.4\times10^6$ ($2.8\times10^5$) and $6.5\times10^6$ ($1.5\times10^6$), respectively.

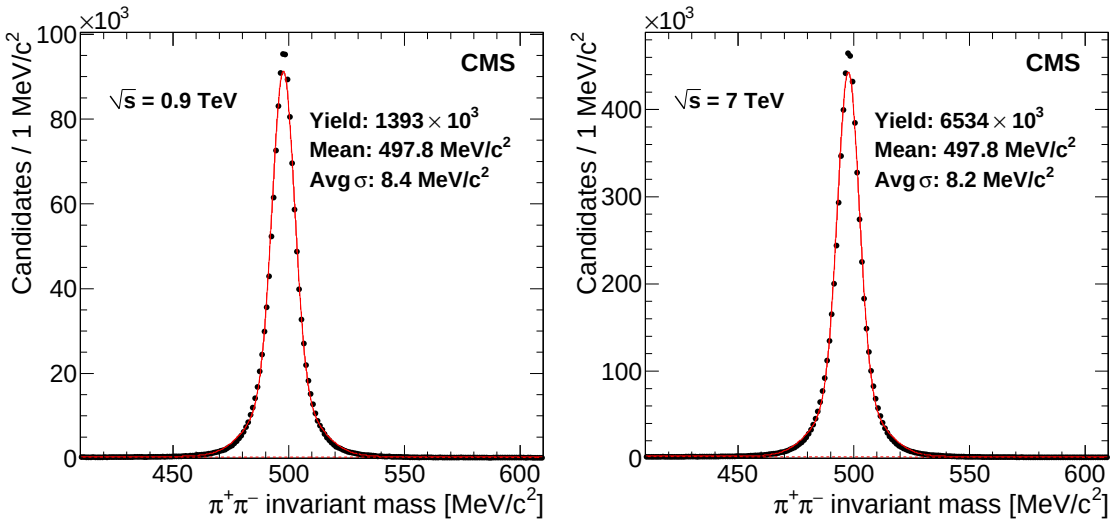


Figure 1: The $\pi^+\pi^-$ invariant mass distributions from data collected at $\sqrt{s} = 0.9$ TeV (left) and 7 TeV (right). The solid curves are fits to a double Gaussian and quadratic polynomial. The dashed curves show the quadratic background contribution.

To reconstruct the $\Xi^-$, charged tracks of the correct sign are combined with $\Lambda$ candidates. The $\chi^2$ probability of the fit to a common vertex for the $\Lambda$ and the charged track must be greater than 5%. In this fit, the $\Lambda$ candidate is constrained to have the correct world-average mass [16]. The primary vertex is refit for each $\Xi^-$ candidate, removing all tracks associated with the $\Xi^-$. The $\Xi^-$ candidates must then pass the following selection criteria:

- 3D impact parameter with respect to the primary vertex $> 2\sigma$ for the proton track from the $\Lambda$ decay, $> 3\sigma$ for the $\pi^-$ track from the $\Lambda$ decay, and $> 4\sigma$ for the $\pi^-$ track from the $\Xi^-$ decay,
- invariant mass from the $\pi^+\pi^-$ hypothesis for the tracks associated with the $\Lambda$ candidate at least 20 MeV/$c^2$ away from the world-average $K^0_S$ mass,
- 3D impact parameter of the $\Xi^-$ candidate with respect to the primary vertex $< 3\sigma$,
- 3D separation between $\Lambda$ vertex and primary vertex $> 10\sigma$, and
- 3D separation between $\Xi^-$ vertex and primary vertex $> 2\sigma$.

The mass distributions of $\Xi^-$ candidates from the $\sqrt{s} = 0.9$ and 7 TeV data are shown in Fig. 3. The $\Lambda\pi^-$ mass is fit with a double Gaussian (with a common mean) signal function and a

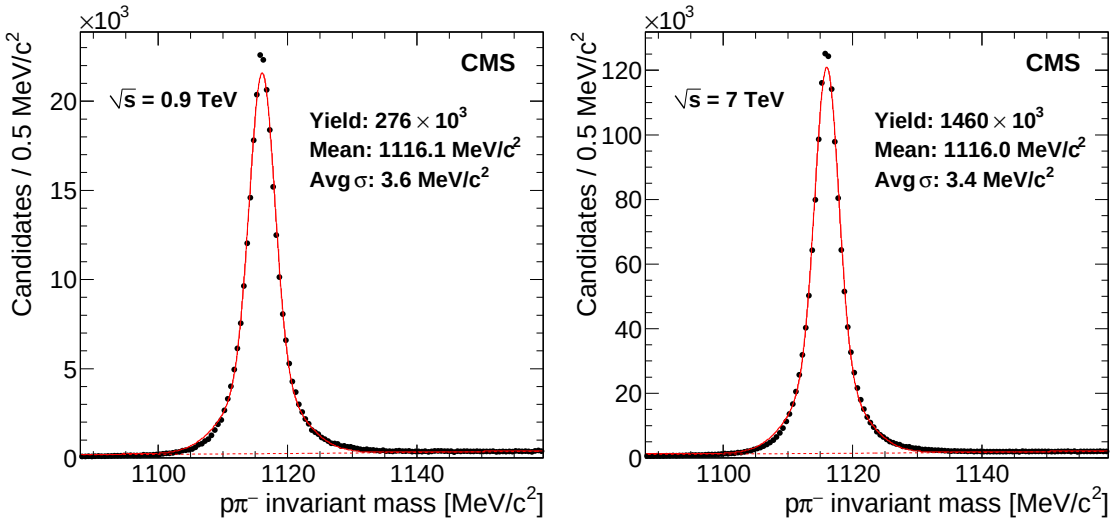


Figure 2: The $p\pi^-$ invariant mass distributions from data collected at $\sqrt{s} = 0.9$ TeV (left) and 7 TeV (right). The solid curves are fits to a double Gaussian signal and a background function given by $Aq^B$, where $q = M_{p\pi^-} - (m_p + m_{\pi^-})$. The dashed curves show the background contribution.

background function of the form $Aq^{1/2} + Bq^{3/2}$, where $q = M_{\Lambda\pi^-} - (m_\Lambda + m_{\pi^-})$ and $M_{\Lambda\pi^-}$ is the $\Lambda\pi^-$ invariant mass. The fitted $\Xi^-$ yields at $\sqrt{s} = 0.9$ and 7 TeV are $6.2\times10^3$ and $3.4\times10^4$, respectively.

## 4 Efficiency correction

The efficiency correction is determined from a Monte Carlo simulation which is used to measure the effects of acceptance and the efficiency for event selection (including the trigger) and particle reconstruction. The Monte Carlo samples are reweighted to match the observed track multiplicity in data, as this has been shown to be an important component of the trigger efficiency [1, 2]. This is referred to as track weighting. The efficiency correction also accounts for the other decay channels of the strange particles that we do not attempt to reconstruct, such as $K^0_S \to \pi^0\pi^0$.

The efficiency is given by the number of reconstructed particles divided by the number of generated particles, subject to two modifications. Firstly, the efficiency correction is used to account for candidates from SD events. As the results are normalized to NSD events, candidates from SD events which pass the event selection must be removed. This is done by defining the efficiency as the number of reconstructed candidates in all events divided by the number of generated candidates in NSD events. Secondly, the efficiency is modified to account for the small contribution of reconstructed non-prompt strange particles which pass the selection criteria. This is only an issue for the $\Lambda$ particles which receive contributions from $\Xi$ and $\Omega$ decays. Since these non-prompt $\Lambda$ particles are present in both the MC and data, we modify the efficiency to remove this contribution by calculating the numerator using all of the reconstructed strange particles and the denominator with only the prompt generated strange particles. As the MC fails to produce enough $\Xi$ particles (see Section 6), the non-prompt $\Lambda$'s are weighted more than prompt $\Lambda$'s in the efficiency calculation.

The results of this analysis are presented in terms of two kinematic distributions: transverse

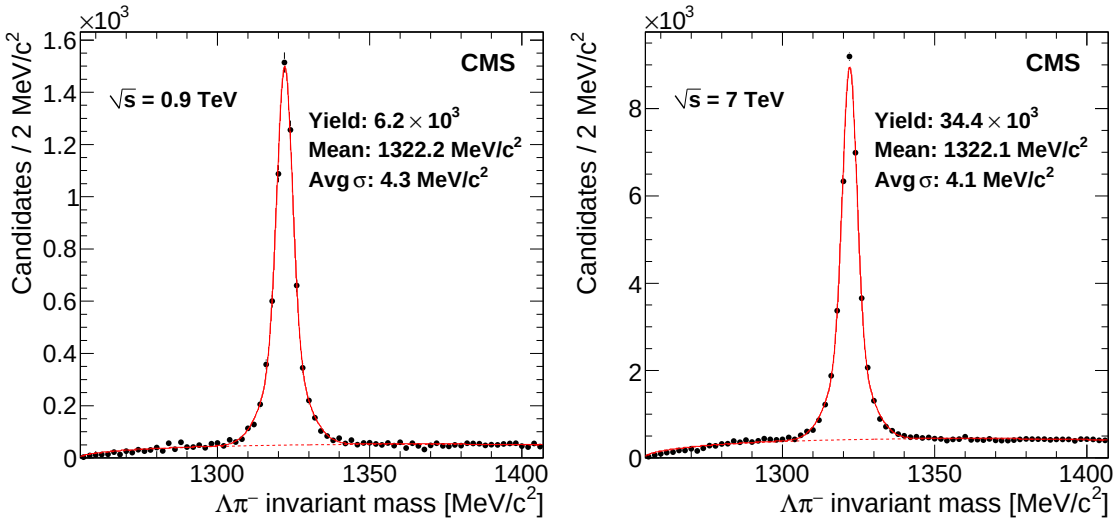


Figure 3: The $\Lambda\pi^-$ invariant mass distributions from data collected at $\sqrt{s} = 0.9$ TeV (left) 7 TeV (right). The solid curves are fits to a double Gaussian signal and a background function given by $Aq^{1/2} + Bq^{3/2}$, where $q = M_{\Lambda\pi^-} - (m_\Lambda + m_{\pi^-})$. The dashed curves show the background contribution.

momentum and rapidity. For all modes, $|y|$ is divided into 10 equal size bins from 0 to 2 and $p_T$ is divided into 20 equal size bins from 0 to 4 GeV/$c$ plus one bin each from 4 to 5 GeV/$c$ and 5 to 6 GeV/$c$. In addition, the $V^0$ modes also have 6–8 GeV/$c$ and 8–10 GeV/$c$ $p_T$ bins. All results are for particles with $|y| < 2$.

The efficiency correction for the $V^0$ modes uses a two-dimensional binning in $p_T$ and $|y|$. Thus, the data are divided into 240 bins in the $|y|, p_T$ plane. The invariant mass histograms in each bin are fit to a double Gaussian signal function (with a common mean) and a background function. In bins with few entries, a single Gaussian signal function is used. For the $\Lambda$ sample, some bins are merged due to sparse populations in $|y|, p_T$ space. The merging is performed separately when measuring $|y|$ and $p_T$ such that the merging occurs across $p_T$ and $|y|$ bins, respectively. The efficiency from MC is evaluated in each bin and applied to the measured yield to obtain the corrected yield. The two-dimensional binning used for the $V^0$ efficiency correction greatly reduces problems arising from remaining differences in production dynamics between the data and the simulation. The much smaller sample of $\Xi^-$ candidates prevents the use of 2D binning. Thus, the data are divided into $|y|$ bins to measure the $|y|$ distribution and into $p_T$ bins to measure the $p_T$ distribution. However, the MC spectra do not match the data. Therefore, each Monte Carlo $\Xi^-$ particle is weighted in $p_T$ ($|y|$) to match the distribution in data when measuring the efficiency versus $|y|$ ($p_T$). Thus, the MC and data distributions are forced to match in the variable over which we integrate to determine the efficiency. We refer to this as kinematic weighting. The efficiencies for all three particles are shown versus $|y|$ and $p_T$ in Fig. 4. The efficiencies (for particles with $|y| < 2$) include the acceptance, event selection, reconstruction and selection, and also account for other decay channels. The increase in efficiency with $p_T$ is due to the improvement in tracking efficiency as track $p_T$ increases and to the selection criteria designed to remove prompt decays. The slight decrease at high $p_T$ is due to particles decaying too far out to have reconstructed tracks. While there is no centre-of-mass energy dependence on the efficiency versus $p_T$, particles produced at $\sqrt{s} = 7$ TeV have a higher average-$p_T$, resulting in a higher efficiency when plotted versus rapidity.

As a check on the ability of the Monte Carlo simulation to reproduce the efficiency, the (well-

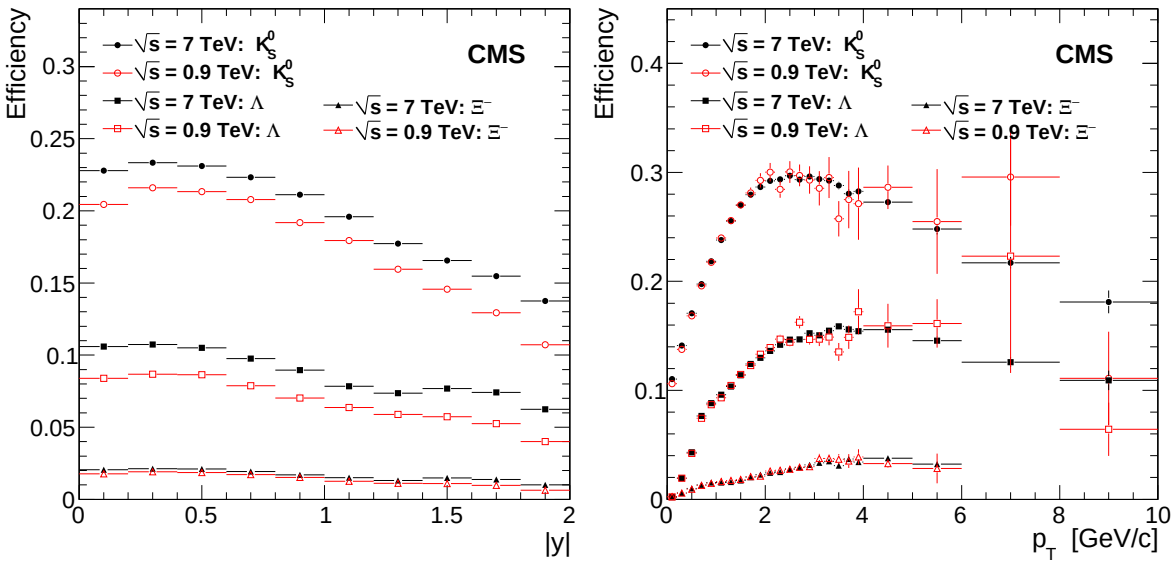


Figure 4: Total efficiencies, including acceptance, trigger and event selection, reconstruction and particle selection, and other decay modes, as a function of $|y|$ (left) and $p_{\mathrm{T}}$ (right) for $\mathrm{K}^0_{\mathrm{S}}$, $\Lambda$, and $\Xi^-$ produced promptly in the range $|y| < 2$. Error bars come from MC statistics.

known) $\mathrm{K}^0_{\mathrm{S}}$, $\Lambda$, and $\Xi^-$ lifetimes are measured. For the $\mathrm{K}^0_{\mathrm{S}}$ measurement, the data are divided into bins of $p_{\mathrm{T}}$ and $ct$, where $ct$ is calculated as $ct = cmL/p$ where $m$, $L$, and $p$ are, respectively, the mass, decay length, and momentum of the particle. In each bin the data is corrected by the MC efficiency and the corrected yields summed in $p_{\mathrm{T}}$ to obtain the $ct$ distribution. Due to smaller sample sizes, the $\Lambda$ and $\Xi^-$ yields are only measured in bins of $ct$. Using the kinematic weighting technique, the MC efficiency in each bin of $ct$ is calculated with the $p_{\mathrm{T}}$ spectrum correctly weighted to match data. The corrected lifetime distributions, shown in Fig. 5, display exponential behaviour. The vertex separation requirements result in very low efficiencies and low yields in the first lifetime bin and are thus expected to have some discrepancies. An actual measurement of the lifetime would remove this issue by using the reduced proper time, where one measures the lifetime relative to the point at which the particle had a chance to be reconstructed. The measured values of the lifetimes are also reasonably consistent with the world averages [16] (shown in Fig. 5) considering that only statistical uncertainties are reported and that this is not the optimal method for a lifetime measurement.

To convert the efficiency corrected yields to per event yields requires the true number of NSD events, which is obtained by correcting the number of selected events for the event selection inefficiency. The event selection includes both the online trigger and offline selection described in Section 2. The event selection efficiency is determined in two ways. In the default method, it is calculated directly from the Monte Carlo simulation (appropriately weighted by the track multiplicity to reproduce the data). In the alternative method, the event selection efficiency versus track multiplicity is derived from the Monte Carlo. Then, each measured event is weighted by the inverse of the event selection efficiency based on its number of tracks. The number of events divided by the number of weighted events gives the event selection efficiency. However, since the event selection requires a primary vertex, no events will have fewer than two tracks. Therefore, the Monte Carlo is also used to determine the fraction of NSD events which have fewer than two tracks and the event selection efficiency is adjusted to include this effect. In both methods, the event selection efficiency accounts for unwanted SD events which pass the event selection. The numerator in the efficiency ratio contains all selected events, including

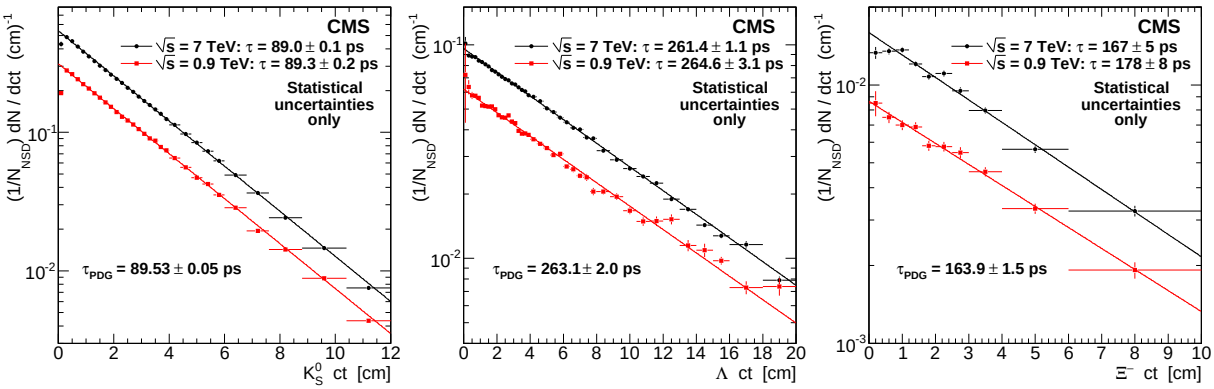


Figure 5: $K^0_S$ (left), $\Lambda$ (middle), and $\Xi^-$ (right) corrected decay time distributions at $\sqrt{s} = 0.9$ and 7 TeV. The values of the lifetimes, derived from a fit with an exponential function (solid line), are shown in the legend along with the world-average value. The error bars and uncertainties on the lifetimes refer to the statistical uncertainty only.

single-diffractive events, while the denominator contains all NSD events.

## 5 Systematic uncertainties

The systematic uncertainties, reported in Table 1, are divided into two categories: normalization uncertainties, which only affect the overall normalization, and point-to-point uncertainties, which may also affect the shape of the $p_T$ and $|y|$ distributions.

The list below summarizes the source and evaluation of the point-to-point systematic uncertainties.

- Kinematic weighting versus 2D binning: The efficiency corrections using the 1D kinematic weighting technique (used for the $\Xi^-$ analysis) and the 2D binning technique (used for the $V^0$ analysis) were compared by measuring the efficiency with both methods on the highest statistics channel ($K^0_S$ at 7 TeV).
- Non-prompt $\Lambda$: The contribution of non-prompt $\Lambda$ decays is varied by a factor of two in the simulation.
- MC tune: The nominal efficiency calculated from the default PYTHIA 6 D6T tune [13] is compared to the efficiency obtained from the PYTHIA 6 Perugia0 (P0) tune [17] and PYTHIA 8 [18].
- Variation of reconstruction cuts: The following cuts are varied for all three modes: $V^0$ vertex separation significance ($\pm 2\sigma$), 3D impact parameter of $V^0$ and $\Xi^-$ ($\pm 2\sigma$), 3D impact parameter of tracks ($\pm 2\sigma$), cut on $K^0_S(\Lambda)$ mass for $\Lambda(K^0_S)$ candidates ($\pm 1.5\sigma$), and increase of number of hits required on each track from 3 to 5. For the $\Xi^-$, additional cuts were varied: the $\Xi^-$ vertex separation significance ($\pm 1\sigma$) and $\Xi^-$ vertex fit probability ($\pm 3\%$).
- Detached particle reconstruction: Finding that the corrected lifetime distributions are exponential with the correct lifetime is a verification of our understanding of the reconstruction efficiency versus decay length. The systematic uncertainty is taken as the difference between the fitted lifetimes and the world-average lifetimes [16]. While the $K^0_S$ and $\Lambda$ lifetimes are within 1% of the world-average, a 2% systematic uncertainty is conservatively assigned.

- Mass fits: As an alternative to using a double-Gaussian signal shape, the $V^0$ invariant mass distributions are fit using a signal shape taken from Monte Carlo.
- Matching versus fitting: The number of reconstructed events, used in the numerator of the efficiency, is calculated in two ways. The truth matching method counts all reconstructed candidates which are matched to a generated candidate, based on the daughter momentum vectors and the decay vertex. The fitting method fits the MC mass distributions to extract a yield. The difference between these two is taken as a systematic.
- Misalignment: The nominal efficiency, obtained using a realistic alignment in the MC, is compared to the efficiency from a MC sample with perfect alignment.
- Beamspot: The location and width of the luminous region of pp collisions (beamspot) is varied in the simulation to assess the effect on efficiency.
- Detector material: The nominal efficiency is compared to the efficiency from a MC simulation in which the tracker was modified. The modification consisted of two parts. First, the mass of the tracker was increased by 5% which is a conservative estimate of the uncertainty. Second, the amounts of the various materials inside the tracker were adjusted within estimated uncertainties to obtain the tracker which maximized the interaction cross section. Both effects were implemented by changing material densities such that the tracker geometry remained the same. The effect is to decrease the efficiency as more particles, both primary and secondary, interact.
- GEANT 4 cross sections: The cross sections used by GEANT 4 for low energy strange baryons and all antibaryons are known to be overestimated [19]. The size of this effect is evaluated by analyzing $\Lambda$–$\overline{\Lambda}$ asymmetries.

As the trigger efficiency is used to derive the number of NSD events, it only affects the normalization. The normalization systematic uncertainties, most of which come from trigger efficiency uncertainties, are described below.

- Alternative trigger efficiency calculation: The difference between the default and alternative trigger efficiency measurements, described in Sec. 4, is taken as the systematic uncertainty on the method.
- Fraction of SD vs NSD: The change in trigger efficiency when the fraction of single-diffractive events in Monte Carlo is varied by $\pm 50\%$ is taken as the systematic uncertainty on the fraction of SD events. The PYTHIA 6 MC produces approximately 20% SD events while the fraction in the triggered data is considerably less [1, 2]. As the UA5 experiment measured 15.5% for this fraction at 900 GeV [20], a variation of $\pm 50\%$ is conservative.
- Modelling diffractive events: In addition to the fraction of SD events, the modelling of SD and NSD events may not be correct. The trigger efficiency obtained using the D6T tune is compared with the trigger efficiency from the P0 tune and PYTHIA 8. In particular, PYTHIA 8 uses a new Pomeron description of diffraction, modelled after PHOJET [21, 22], which results in a large increase in the track multiplicity of SD events.
- Track weighting: The track weighting of the Monte Carlo primarily affects the trigger efficiency. The track weighting requires a measurement of the track multiplicity distribution in data and MC. The default track multiplicity distribution is calculated from events which pass the trigger, except the primary vertex requirement is not applied. Two variations are considered. First, the track multiplicity distribution is

measured from events also requiring a primary vertex. As this requires at least two tracks per event, the weight for events with fewer than two tracks is taken to be the same as the weight for events with two tracks. Second, the track weighting is determined with the primary vertex requirement (as in the first case), but without the HF trigger. The variation is taken as a systematic uncertainty on the track weighting.

- Branching fractions: The results are corrected for other decay channels of $K^0_S$, $\Lambda$, and $\Xi^-$. The branching fraction uncertainty reported by the PDG [16] is used as the systematic uncertainty.

The systematic uncertainties at the two centre-of-mass energies are found to be essentially the same. The normalization uncertainties and the detached particle reconstruction uncertainty are obtained from the average of the results from the two centre-of-mass energies. The other point-to-point systematic uncertainties are derived from the higher statistics 7 TeV results. The point-to-point systematic uncertainties are measured as functions of $p_T$ and $|y|$ and found to be independent of both variables. Therefore, the systematic uncertainties are estimated such that they include approximately 68% of the points (representing a $1\sigma$ error). The resulting systematic uncertainties are summarized in Table 1.

Table 1: Systematic uncertainties for the $K^0_S$, $\Lambda$, and $\Xi^-$ production measurements.

| Source | $K^0_S$ (%) | $\Lambda$ (%) | $\Xi^-$ (%) |
|---|---|---|---|
| Point-to-point systematic uncertainties | | | |
| Kinematic weight vs. 2D binning | 1.0 | 1.0 | 1.0 |
| Non-prompt $\Lambda$ | — | 3.0 | — |
| MC tune | 2.0 | 3.0 | 4.0 |
| Reconstruction cuts | 4.0 | 5.0 | 5.0 |
| Detached particle reconstruction | 2.0 | 2.0 | 3.5 |
| Mass fits | 0.5 | 2.0 | 2.0 |
| Matching vs. fitting | 2.0 | 3.0 | 3.0 |
| Misalignment | 1.0 | 1.0 | 1.0 |
| Beamspot | 1.0 | 1.5 | 2.0 |
| Detector material | 2.0 | 5.0 | 8.0 |
| GEANT 4 cross sections | 0.0 | 5.0 | 5.0 |
| Point-to-point sum | 5.9 | 10.7 | 12.7 |
| Normalization systematic uncertainties | | | |
| Trigger calculation | 1.8 | 1.8 | 1.8 |
| SD fraction | 2.8 | 2.8 | 2.8 |
| Diffractive modelling | 1.5 | 1.5 | 1.5 |
| Track weighting | 2.0 | 2.0 | 2.0 |
| Branching fractions | 0.1 | 0.8 | 0.8 |
| Normalization sum | 4.1 | 4.2 | 4.2 |
| Overall sum | 7.2 | 11.5 | 13.4 |

For the measurements of $dN/dy$, $dN/dy|_{y\approx 0}$, and $dN/dp_T$, the full systematic uncertainty is applied. For the $\Lambda/K^0_S$ and $\Xi^-/\Lambda$ production ratio measurements, the largest point-to-point systematic uncertainty of the two particles is used and, among the normalization systematic uncertainties, only the branching fraction correction is considered. Note that for the $\Xi^-/\Lambda$ production ratios, the $\Lambda$ branching fraction uncertainty cancels in the ratio.

# 6 Results

The results reported here are normalized to NSD interactions. The number of NSD raw events (given in Sec. 2) are corrected for the trigger efficiency and the fraction of SD events after the selection. The corrected number of NSD events is $9.95 \times 10^6$ and $37.10 \times 10^6$ for $\sqrt{s} = 0.9$ and 7 TeV, respectively.

## 6.1 Distributions $dN/dy$ and $dN/dp_{\mathrm{T}}$

The corrected yields of $\mathrm{K}^0_{\mathrm{S}}$, $\Lambda$, and $\Xi^-$, versus $|y|$ and $p_{\mathrm{T}}$ are plotted in Fig. 6, normalized to the number of NSD events. The rapidity distribution is flat at central rapidities with a slight decrease at higher rapidities while the $p_{\mathrm{T}}$ distribution is observed to be rapidly falling. The rapidity distributions also show results from three different PYTHIA models: PYTHIA 6.422 with the D6T and P0 tunes [13, 17] and PYTHIA 8.135 [18]. Fits to the Tsallis function, described below, are overlaid on the $p_{\mathrm{T}}$ distributions.

## 6.2 Analysis of $p_{\mathrm{T}}$ spectra

The corrected $p_{\mathrm{T}}$ spectra are fit to the Tsallis function [23], as was done for charged particles [1, 2]. The Tsallis function used is:

$$\frac{1}{N_{\mathrm{NSD}}}\frac{dN}{dp_{\mathrm{T}}} = C\frac{(n-1)(n-2)}{nT[nT+m(n-2)]}p_{\mathrm{T}}\left[1+\frac{\sqrt{p_{\mathrm{T}}^2+m^2}-m}{nT}\right]^{-n}, \tag{1}$$

where $C$ is a normalization parameter and $T$ and $n$ are the shape parameters. The results of the fits are shown in Table 2. The data points used in the fits include only the statistical uncertainty. The statistical uncertainties on the fit parameters are obtained from the fit. The systematic uncertainties are obtained by varying the cuts and Monte Carlo conditions (tune, material, beamspot, and alignment) in the same way as used to obtain the point-to-point systematic uncertainties on the distributions. The systematic uncertainty on the normalization parameter $C$ also includes the normalization uncertainty given in Table 1. The normalized $\chi^2$ indicates good fits to most of the samples. The $T$ parameter can be associated with the inverse slope parameter of an exponential which dominates at low $p_{\mathrm{T}}$, while the $n$ parameter controls the power law behaviour at high $p_{\mathrm{T}}$. While both parameters are necessary, they are highly correlated, with correlation coefficients around 0.9, making it difficult to elucidate information. Nevertheless, it is clear that $T$ increases with particle mass and centre-of-mass energy. This indicates a broader low-$p_{\mathrm{T}}$ shape at higher centre-of-mass energy and for higher mass particles. In contrast, the high $p_{\mathrm{T}}$ power-law behaviour seems to show a much steeper fall off for the two baryons than for the $\mathrm{K}^0_{\mathrm{S}}$. While the power-law behaviour of the baryons does not show any dependence on the centre-of-mass energy, the fall off of the $\mathrm{K}^0_{\mathrm{S}}$ particles produced at $\sqrt{s} = 0.9$ TeV is steeper than those produced at $\sqrt{s} = 7$ TeV.

We calculate the average $p_{\mathrm{T}}$ directly from the data in the $dN/dp_{\mathrm{T}}$ histograms. The Tsallis function fit is used to obtain the correct bin centre and to account for events beyond the measured $p_{\mathrm{T}}$ range, both of which are small effects. The statistical uncertainty on the average $p_{\mathrm{T}}$ is obtained by finding the standard deviation of $p_{\mathrm{T}}$ and dividing by the square root of the equivalent number of background-free events, where the equivalent number of background-free events is given by the square of the inverse of the relative uncertainty on the total number of signal events. The systematic uncertainty is composed of two components added in quadrature. The first component is the same as used in determining the Tsallis function systematic uncertainties (varying the cuts and Monte Carlo conditions). The second component is obtained by using the

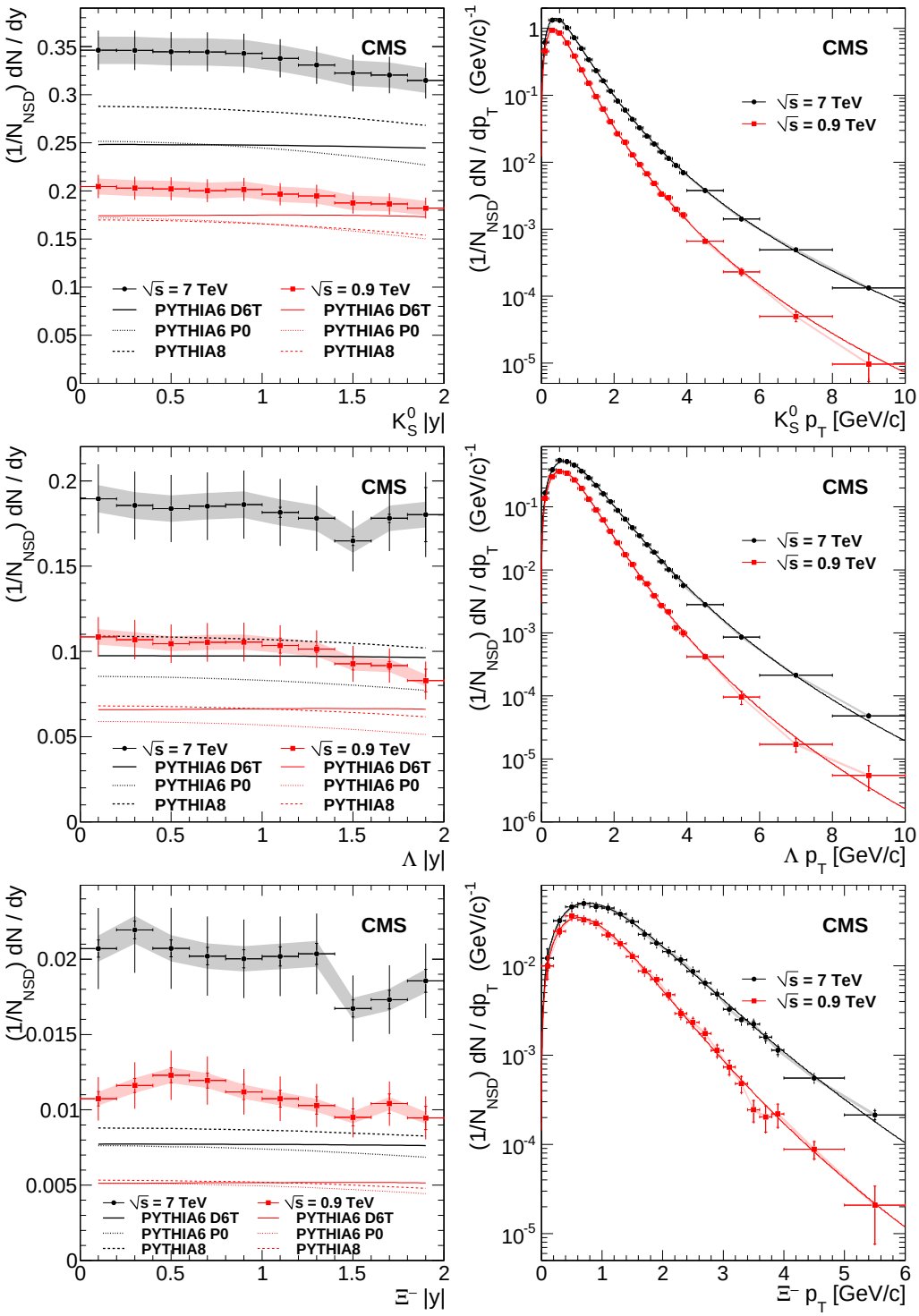


Figure 6: $K^0_S$ (top), $\Lambda$ (middle), and $\Xi^-$ (bottom) production per NSD event versus $|y|$ (left) and $p_T$ (right). The inner vertical error bars (when visible) show the statistical uncertainties, the outer the statistical and point-to-point systematic uncertainties summed in quadrature. The normalization uncertainty is shown as a band. Three PYTHIA predictions are overlaid on the $|y|$ distributions. The solid curves in the $p_T$ distributions are fits to the Tsallis function as described in the text.

Table 2: Results of fitting the Tsallis function to the data. In the $C$, $T$, and $n$ columns, the first uncertainty is statistical and the second is systematic. The parameter values and $\chi^2$/NDF are obtained from fits to the data with only the statistical uncertainty included.

| Particle | $\sqrt{s}$ (TeV) | $C$ | $T$ (MeV) | $n$ | $\chi^2$/NDF |
|---|---|---|---|---|---|
| $K^0_S$ | 0.9 | $0.776 \pm 0.002 \pm 0.042$ | $187 \pm 1 \pm 4$ | $7.79 \pm 0.07 \pm 0.26$ | 19/21 |
| $\Lambda$ | 0.9 | $0.395 \pm 0.002 \pm 0.041$ | $216 \pm 2 \pm 11$ | $9.3 \pm 0.2 \pm 1.1$ | 32/21 |
| $\Xi^-$ | 0.9 | $0.043 \pm 0.001 \pm 0.006$ | $250 \pm 8 \pm 48$ | $10.1 \pm 0.9 \pm 4.7$ | 19/19 |
| $K^0_S$ | 7 | $1.329 \pm 0.001 \pm 0.062$ | $220 \pm 1 \pm 3$ | $6.87 \pm 0.02 \pm 0.09$ | 50/21 |
| $\Lambda$ | 7 | $0.696 \pm 0.002 \pm 0.058$ | $292 \pm 1 \pm 10$ | $9.3 \pm 0.1 \pm 0.5$ | 128/21 |
| $\Xi^-$ | 7 | $0.080 \pm 0.001 \pm 0.012$ | $361 \pm 7 \pm 72$ | $11.2 \pm 0.7 \pm 4.9$ | 21/19 |

mean $p_T$ of the fitted Tsallis function. The average $p_T$ from data and PYTHIA 6 with the D6T underlying event tune is shown in Table 3. The PYTHIA values are quite close to the $\sqrt{s} = 7$ TeV data and somewhat lower than the $\sqrt{s} = 0.9$ TeV data. Although the average $p_T$ results from PYTHIA are relatively close to the data, the PYTHIA $p_T$ distributions are significantly broader than the data distributions. This disagreement can be seen in Fig. 7, which shows the ratio of PYTHIA to data for production of $K^0_S$, $\Lambda$, and $\Xi^-$ versus transverse momentum. As well as a broader distribution, the PYTHIA distributions also show significant variation as a function of tune and version.

Table 3: Average $p_T$ in units of MeV/$c$ obtained from the appropriate $dN/dp_T$ distribution as described in the text. Results from PYTHIA 6 with tune D6T are also given. In each data column, the first uncertainty is statistical and the second is systematic.

| | $\sqrt{s} = 0.9$ TeV | | $\sqrt{s} = 7$ TeV | |
|---|---|---|---|---|
| Particle | Data | MC (D6T) | Data | MC (D6T) |
| $K^0_S$ | $654 \pm 1 \pm 8$ | 580 | $790 \pm 1 \pm 9$ | 757 |
| $\Lambda$ | $837 \pm 6 \pm 40$ | 750 | $1037 \pm 5 \pm 63$ | 1071 |
| $\Xi-$ | $971 \pm 14 \pm 43$ | 831 | $1236 \pm 11 \pm 72$ | 1243 |

The relative production versus transverse momentum between different species is shown in Fig. 8. The $N(\Lambda)/N(K^0_S)$ and $N(\Xi^-)/N(\Lambda)$ distributions both increase with $p_T$ at low $p_T$, as expected from the higher average $p_T$ for the higher mass particles. At higher $p_T$ the $N(\Lambda)/N(K^0_S)$ distribution drops off while the $N(\Xi^-)/N(\Lambda)$ distribution appears to plateau. This is consistent with the values of the power-law parameter $n$ for these distributions. Interestingly, the collision energy has no observable effect on the level or shape of these production ratios. The PYTHIA results are superimposed on the same plot. While PYTHIA reproduces the general features, it differs significantly in the details and shows large variations depending on tune and version.

Figure 9 shows a comparison of the CMS $p_T$ distributions with results from other recent experiments [3, 24, 25]. To compare with the CMS results, the CDF, ALICE, and STAR distributions are multiplied by $8\pi p_T$, 4, and $8\pi$, respectively. The CDF cross sections are also divided by 49 mb (the NSD cross section used by CDF [25]) to obtain distributions normalized to NSD events, matching the CMS and STAR normalization. The ALICE results are normalized to inelastic events (including single diffractive events). The ALICE and CMS results at 0.9 TeV agree for all three particles. The distributions behave as expected, with higher centre-of-mass energy corresponding to increased production rates and harder spectra. To remove the effect of normalization, Fig. 10 shows a comparison of $\Lambda$ to $K^0_S$ and $\Xi^-$ to $\Lambda$ production ratios versus transverse momentum. The CMS results agree with the results from pp collisions at $\sqrt{s}$ =0.2 TeV

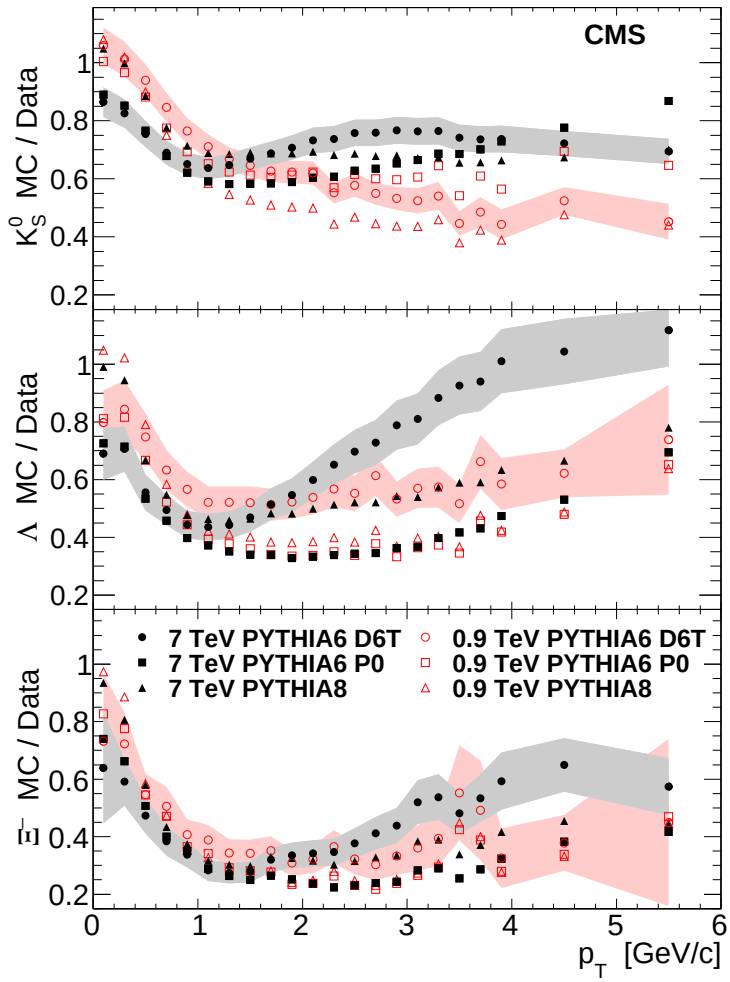


Figure 7: Ratio of MC production to data production of $K^0_S$ (top), $\Lambda$ (middle), and $\Xi^-$ (bottom) versus $p_T$ at $\sqrt{s} = 0.9$ TeV (open symbols) and $\sqrt{s} = 7$ TeV (filled symbols). Results are shown for three PYTHIA predictions at each centre-of-mass energy. To reduce clutter, the uncertainty, shown as a band, is included for only one of the predictions (D6T) at each energy. This uncertainty includes the statistical and point-to-point systematic uncertainties added in quadrature but does not include the normalization systematic uncertainty.

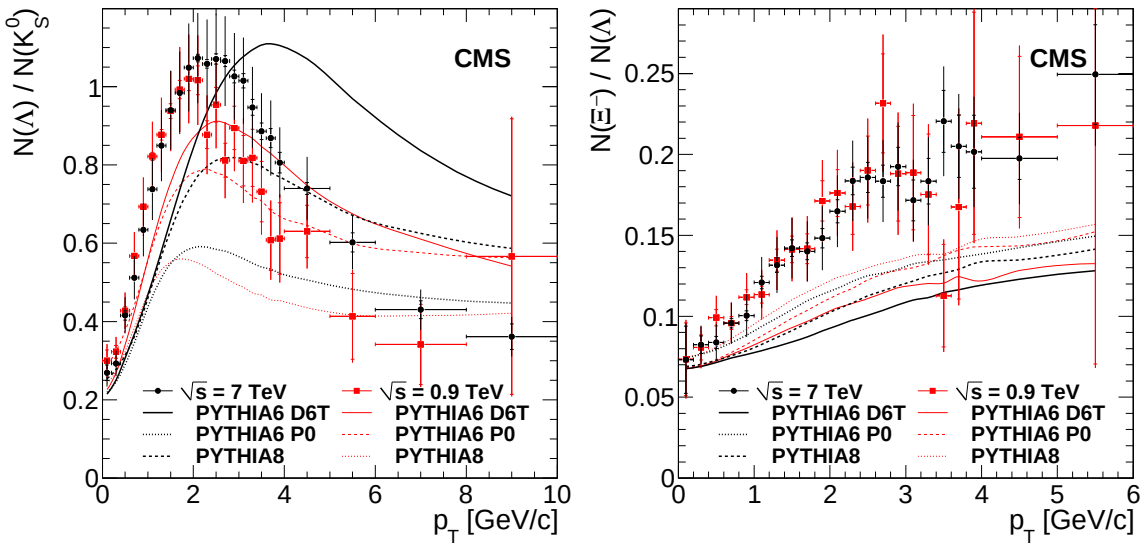


Figure 8: $N(\Lambda)/N(\mathrm{K}^0_\mathrm{S})$ (left) and $N(\Xi^-)/N(\Lambda)$ (right) in NSD events versus $p_\mathrm{T}$. The inner vertical error bars (when visible) show the statistical uncertainties, the outer the statistical and all systematic uncertainties summed in quadrature. Results are shown for three PYTHIA predictions at each centre-of-mass energy.

from STAR [24] and at $\sqrt{s}$ =0.9 TeV results from ALICE [3]. These three results show a remarkable consistency across a wide variety of collision energies. In contrast, the CDF values for $N(\Lambda)/N(\mathrm{K}^0_\mathrm{S})$ [26] are significantly higher than the CMS results while the CDF measurements of $N(\Xi^-)/N(\Lambda)$ [25] are lower, albeit with less significance.

Reducing the $p_\mathrm{T}$ distributions to a single value, the average $p_\mathrm{T}$, we compare the CMS results with earlier results at lower energies in Fig. 11 [3, 24, 26–32]. The CMS results are in excellent agreement with the recent ALICE measurements at 0.9 TeV. The CMS results continue the overall trend of increasing average $p_\mathrm{T}$ with increasing particle mass and increasing centre-of-mass energy.

### 6.3 Analysis of production rate

As a measure of the overall production rate in NSD events, $\frac{dN}{dy}|_{y\approx 0}$ and the total yield for $|y| < 2$ were extracted and tabulated in Table 4. The quantity $\frac{dN}{dy}|_{y\approx 0}$ is the average value of $\frac{dN}{dy}$ over the region $|y| < 0.2$. The integrated yields for $|y| < 2$ are obtained by integrating the $p_\mathrm{T}$ spectra, using the Tsallis function fit to account for particles above the measured $p_\mathrm{T}$ range.

The central production rates of $\mathrm{K}^0_\mathrm{S}$, $\Lambda$, and $\Xi^-$ are compared to previous results in Fig. 12. The results show the expected increase in production with centre-of-mass energy with little evidence of a difference due to beam particles. As the ALICE results are normalized to all inelastic collisions, they are expected to be somewhat lower than the CMS results.

The production ratios $N(\mathrm{K}^0_\mathrm{S})/N(\Lambda)$ and $N(\Xi^-)/N(\Lambda)$ versus $|y|$ are shown in Fig. 13. The rapidity distributions are very flat and, as observed in the $p_\mathrm{T}$ distributions of Fig. 8, show no dependence on centre-of-mass energy. Three PYTHIA predictions at each centre-of-mass energy are also shown in Fig. 13. These results confirm what can already be seen in the comparisons shown in the left panes of Fig. 6; PYTHIA underestimates the production of strange particles and the discrepancy grows with particle mass.

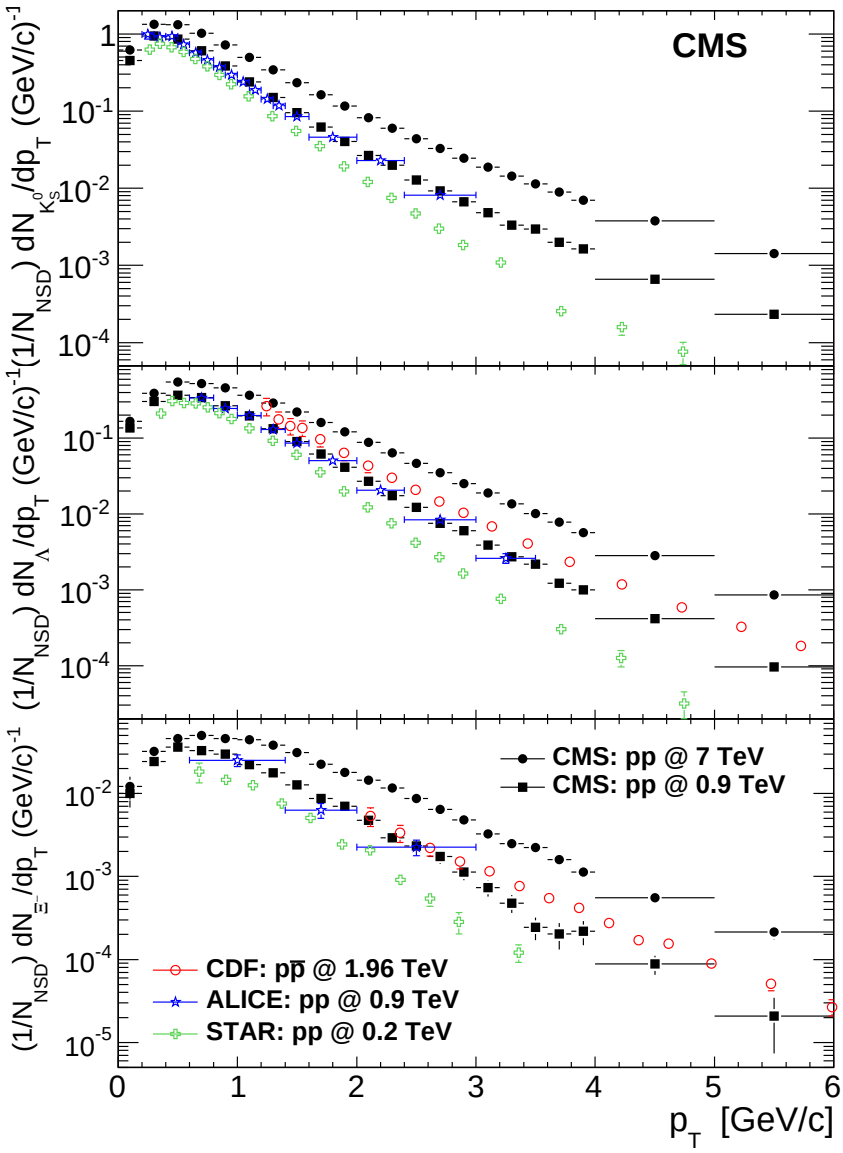


Figure 9: $K^0_S$ (top), $\Lambda$ (middle), and $\Xi^-$ (bottom) production per event versus $p_T$. The error bars on the CMS results show the combined statistical, point-to-point systematic, and normalization systematic uncertainties. The error bars on the CDF [25], ALICE [3], and STAR [24] results show the combined statistical and systematic uncertainties. The CMS, CDF, and STAR results are normalized to NSD events while the ALICE results are normalized to all inelastic events.

Table 4: $\frac{dN}{dy}|_{y\approx 0}$ and integrated yields ($|y| < 2.0$) per NSD event from data. In each data column, the first uncertainty is statistical and the second is systematic.

| Particle | $\sqrt{s} = 0.9$ TeV | | $\sqrt{s} = 7$ TeV | |
|---|---|---|---|---|
| | $\frac{dN}{dy}\|_{y\approx 0}$ | $N$ | $\frac{dN}{dy}\|_{y\approx 0}$ | $N$ |
| $K^0_S$ | $0.205 \pm 0.001 \pm 0.015$ | $0.784 \pm 0.002 \pm 0.056$ | $0.346 \pm 0.001 \pm 0.025$ | $1.341 \pm 0.001 \pm 0.097$ |
| $\Lambda$ | $0.108 \pm 0.001 \pm 0.012$ | $0.404 \pm 0.004 \pm 0.046$ | $0.189 \pm 0.001 \pm 0.022$ | $0.717 \pm 0.005 \pm 0.082$ |
| $\Xi^-$ | $0.011 \pm 0.001 \pm 0.001$ | $0.043 \pm 0.001 \pm 0.006$ | $0.021 \pm 0.001 \pm 0.003$ | $0.080 \pm 0.001 \pm 0.011$ |

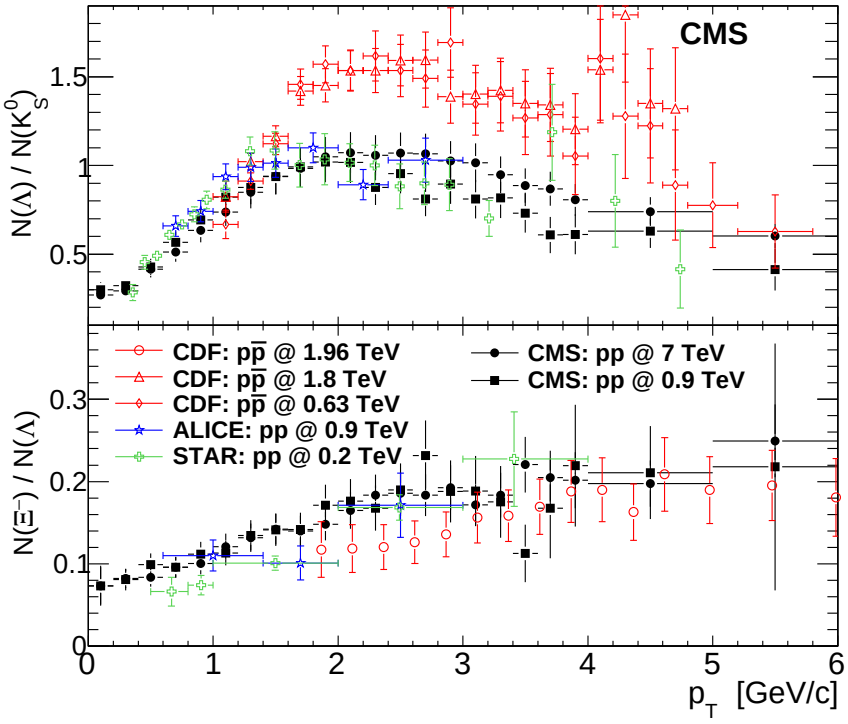


Figure 10: Ratio of $\Lambda$ to $K^0_S$ production (top) and $\Xi^-$ to $\Lambda$ production (bottom) versus $p_T$. The CMS, ALICE [3], and STAR [24] error bars include the statistical and systematic uncertainties. The CDF error bars include the statistical uncertainties for $N(\Lambda)/N(K^0_S)$ [26] and the statistical and systematic uncertainties for $N(\Xi^-)/N(\Lambda)$ [25]. The CDF $N(\Lambda)/N(K^0_S)$ bin sizes are doubled to reduced fluctuations. For experiments in which the binning for $\Lambda$ and $\Xi^-$ is different (ALICE and STAR), bins are merged to provide common bin ranges in the $N(\Xi^-)/N(\Lambda)$ distribution.

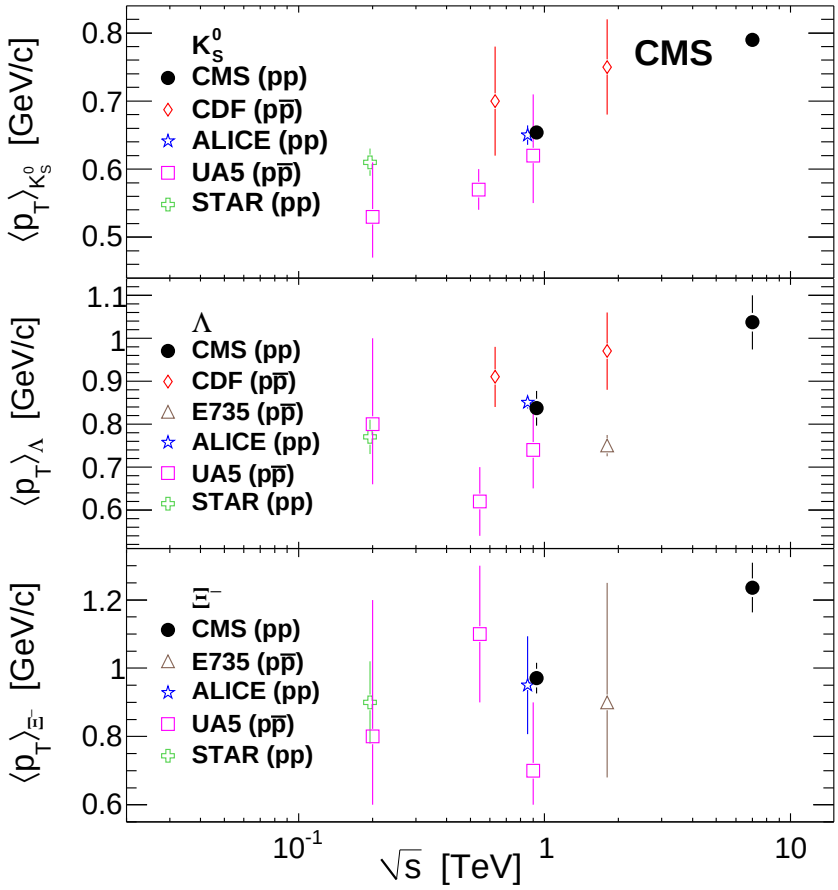


Figure 11: Average $p_T$ for $K^0_S$ (top), $\Lambda$ (middle), and $\Xi^-$ (bottom), as a function of the centre-of-mass energy. The CMS measurements are for $|y| < 2$. The other results are from UA5 [27–31] ($p\bar{p}$ collisions covering $|y| < 2.5$, $|y| < 2$, and $|y| < 3$ for $K^0_S$, $\Lambda$, and $\Xi^-$, respectively), E735 [32] ($p\bar{p}$ collisions using tracks with $-0.36 < \eta < 1.0$), CDF [26] ($p\bar{p}$ collisions covering $|\eta| < 1.0$), STAR [24] (pp collisions covering $|y| < 0.5$), and ALICE [3] (pp collisions covering $|y| < 0.75$ for $K^0_S$ and $\Lambda$ and $|y| < 0.8$ for $\Xi^-$). Some points have been slightly offset from the true energy to improve visibility. The vertical bars indicate the statistical and systematic uncertainties (when available) summed in quadrature.

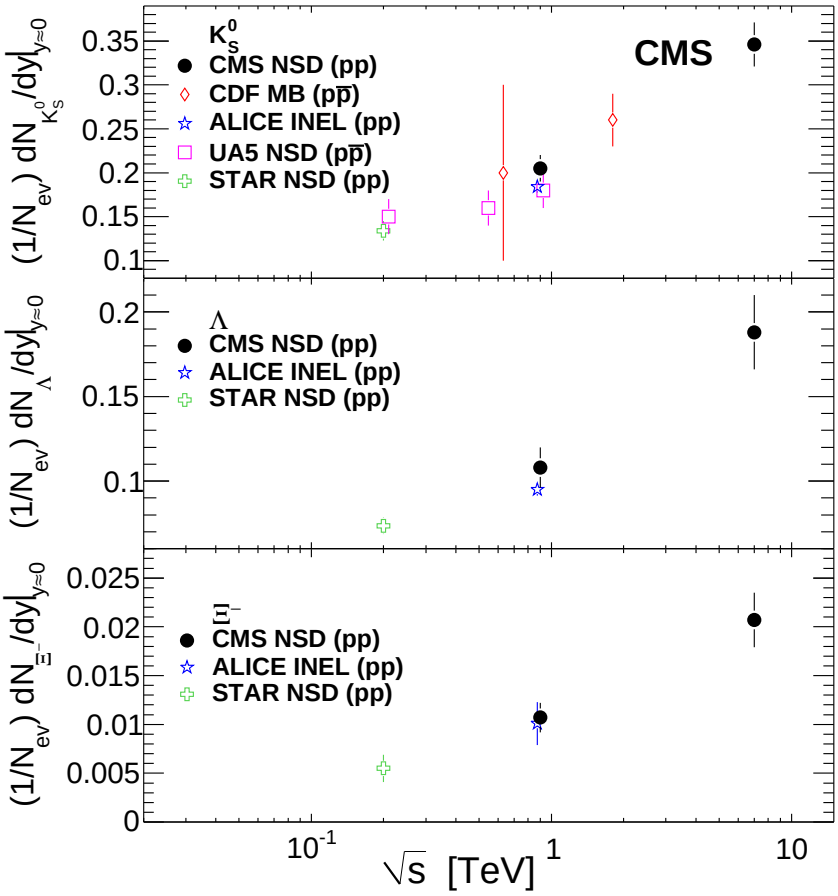


Figure 12: The central rapidity production rate for $K^0_S$ (top), $\Lambda$ (middle), and $\Xi^-$ (bottom), as a function of the centre-of-mass energy. The previous results are from UA5 [29, 30] ($p\bar{p}$), CDF [33] ($p\bar{p}$), STAR [24] (pp), and ALICE [3] (pp). The CMS, UA5, and STAR results are normalized to NSD events. The CDF results are normalized to events passing their trigger and event selection defined chiefly by activity in both sides of the detector, at least four tracks, and a primary vertex. The ALICE results are normalized to all inelastic events. Some points have been slightly offset from the true energy to improve visibility. The vertical bars indicate the statistical uncertainties for the UA5 and CDF results and the combined statistical and systematic uncertainties for the CMS, ALICE, and STAR results.

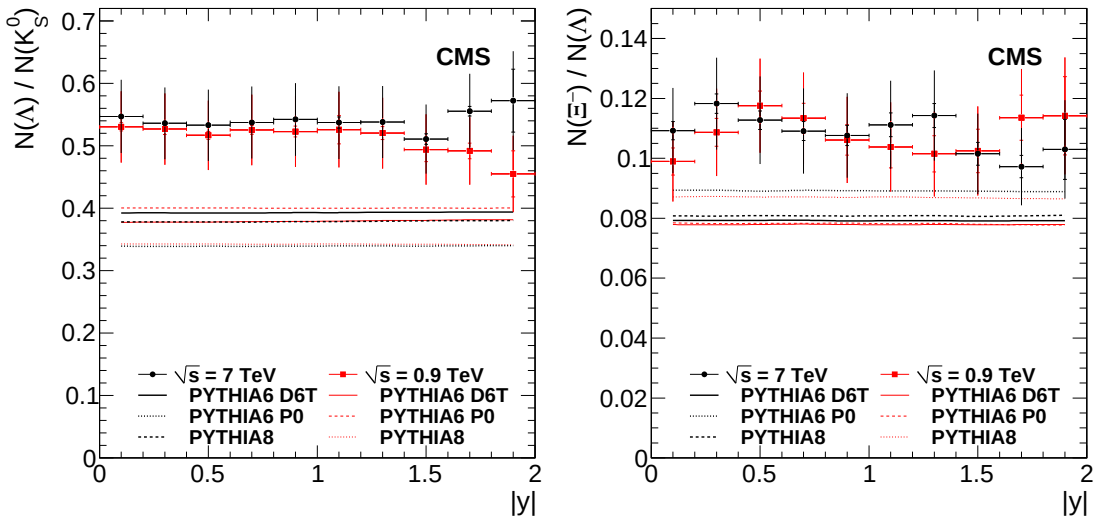


Figure 13: The production ratios $N(\Lambda)/N(\mathrm{K}^0_\mathrm{S})$ (left) and $N(\Xi^-)/N(\Lambda)$ (right) in NSD events versus $|y|$. The inner vertical error bars (when visible) show the statistical uncertainties, the outer the statistical and all systematic uncertainties summed in quadrature. Results are shown for three PYTHIA predictions at each centre-of-mass energy.

Table 5 shows a comparison of the production rate of data to PYTHIA 6 with the D6T tune. The left column shows a large increase in the strange particle production cross section as the centre-of-mass energy increases from 0.9 to 7 TeV. The systematic uncertainties for this ratio are reduced as the same uncertainty affects both samples nearly equally. The results for $\mathrm{K}^0_\mathrm{S}$ and $\Lambda$ are consistent with the increase observed in inclusive charged particle production [1, 2] ($\frac{5.82}{3.48} = 1.67$) while the $\Xi^-$ results show a slightly greater increase. The increase in particle production from 0.9 to 7 TeV is not well modelled by PYTHIA 6. Another feature, seen in the right column, is the deficit of strange particles produced by PYTHIA 6. The deficit of $\mathrm{K}^0_\mathrm{S}$ particles in the MC, 15% (28%) low at 0.9 (7) TeV, is consistent with the results found in the production of charged particles [1, 2]. However, the deficit is much worse as the mass increases, resulting in a 63% reduction in $\Xi^-$ particles in MC compared to data at $\sqrt{s}$ =7 TeV. While values are only presented for PYTHIA 6 with the D6T tune, the same features are also evident for the other two PYTHIA comparisons in the rapidity distribution plots in Fig. 6.

Table 5: Comparison of strangeness production rates between PYTHIA 6 Monte Carlo (D6T) and data. In each column, the first uncertainty is statistical and the second is systematic.

| Particle | $\left[\frac{\frac{dN}{dy}\vert_{y\approx0}(7\,\mathrm{TeV})}{\frac{dN}{dy}\vert_{y\approx0}(0.9\,\mathrm{TeV})}\right]$ | | $\left[\frac{\frac{dN}{dy}\vert_{y\approx0}(\mathrm{MCD6T})}{\frac{dN}{dy}\vert_{y\approx0}(\mathrm{Data})}\right]$ | |
|---|---|---|---|---|
| | Data | MC (D6T) | $\sqrt{s} = 0.9$ TeV | $\sqrt{s} = 7$ TeV |
| $\mathrm{K}^0_\mathrm{S}$ | $1.69 \pm 0.01 \pm 0.06$ | 1.42 | $0.852 \pm 0.005 \pm 0.061$ | $0.717 \pm 0.001 \pm 0.052$ |
| $\Lambda$ | $1.75 \pm 0.02 \pm 0.08$ | 1.48 | $0.606 \pm 0.007 \pm 0.070$ | $0.514 \pm 0.003 \pm 0.059$ |
| $\Xi^-$ | $1.93 \pm 0.10 \pm 0.09$ | 1.51 | $0.477 \pm 0.021 \pm 0.064$ | $0.373 \pm 0.010 \pm 0.050$ |

## 7 Conclusions

This article presents a study of the production of $\mathrm{K}^0_\mathrm{S}$, $\Lambda$, and $\Xi^-$ particles in proton-proton collisions at centre-of-mass energies 0.9 and 7 TeV. By fully exploiting the low-momentum track

reconstruction capabilities of CMS, we have measured the transverse-momentum distribution of these strange particles down to zero. From this sample of 10 million strange particles, the transverse momentum distributions were measured out to 10 GeV/$c$ for $K^0_S$ and $\Lambda$ and out to 6 GeV/$c$ for $\Xi^-$. We fit these distributions with a Tsallis function to obtain information on the exponential decay at low $p_T$ and the power-law behaviour at high $p_T$. All species show a flattening of the exponential decay as the centre-of-mass energy increases. While the baryons show little change in the high-$p_T$ region, the $K^0_S$ power-law parameter decreases from 7.8 to 6.9. The average $p_T$ values, calculated directly from the data, are found to increase with particle mass and centre-of-mass energy, in agreement with predictions and other experimental results. While the PYTHIA $p_T$ distributions used in this analysis show significant variation based on tune and version, they are all broader than the data distributions.

We have also measured the production versus rapidity and extracted the value of $dN/dy$ in the central rapidity region. The increase in production of strange particles as the centre-of-mass energy increases from 0.9 to 7 TeV is approximately consistent with the results for inclusive charged particles. However, as in the inclusive charged particle case, PYTHIA fails to match this increase. For $K^0_S$ production, the discrepancy is similar to what has been found in charged particles. However, the deficit between PYTHIA and data is significantly larger for the two hyperons at both energies, reaching a factor of three discrepancy for $\Xi^-$ production at $\sqrt{s} = 7\,\text{TeV}$. If a quark-gluon plasma or other collective effects were present, we might expect an enhancement of double-strange baryons to single-strange baryons and/or an enhancement of strange baryons to strange mesons. However, the production ratios $N(\Lambda)/N(K^0_S)$ and $N(\Xi^-)/N(\Lambda)$ versus rapidity and transverse momentum show no change with centre-of-mass energy. Thus, the deficiency in PYTHIA is likely originating from parameters regulating the frequency of strange quarks appearing in colour strings. The variety of measurements presented here can be used to tune PYTHIA and other models as well as a baseline to understand measurements of strangeness production in heavy-ion collisions.

## Acknowledgements

We wish to congratulate our colleagues in the CERN accelerator departments for the excellent performance of the LHC machine. We thank the technical and administrative staff at CERN and other CMS institutes, and acknowledge support from: FMSR (Austria); FNRS and FWO (Belgium); CNPq, CAPES, FAPERJ, and FAPESP (Brazil); MES (Bulgaria); CERN; CAS, MoST, and NSFC (China); COLCIENCIAS (Colombia); MSES (Croatia); RPF (Cyprus); Academy of Sciences and NICPB (Estonia); Academy of Finland, ME, and HIP (Finland); CEA and CNRS/IN2P3 (France); BMBF, DFG, and HGF (Germany); GSRT (Greece); OTKA and NKTH (Hungary); DAE and DST (India); IPM (Iran); SFI (Ireland); INFN (Italy); NRF and WCU (Korea); LAS (Lithuania); CINVESTAV, CONACYT, SEP, and UASLP-FAI (Mexico); PAEC (Pakistan); SCSR (Poland); FCT (Portugal); JINR (Armenia, Belarus, Georgia, Ukraine, Uzbekistan); MST and MAE (Russia); MSTD (Serbia); MICINN and CPAN (Spain); Swiss Funding Agencies (Switzerland); NSC (Taipei); TUBITAK and TAEK (Turkey); STFC (United Kingdom); DOE and NSF (USA). Individuals have received support from the Marie-Curie programme and the European Research Council (European Union); the Leventis Foundation; the A. P. Sloan Foundation; the Alexander von Humboldt Foundation; the Associazione per lo Sviluppo Scientifico e Tecnologico del Piemonte (Italy); the Belgian Federal Science Policy Office; the Fonds pour la Formation à la Recherche dans l'índustrie et dans l'Ágriculture (FRIA-Belgium); and the Agentschap voor Innovatie door Wetenschap en Technologie (IWT-Belgium).

## References


[1] CMS Collaboration, "Transverse-momentum and pseudorapidity distributions of charged hadrons in $pp$ collisions at $\sqrt{s}$=0.9 and 2.36 TeV", *JHEP* **02** (2010) 041, arXiv:1002.0621. doi:10.1007/JHEP02(2010)041.

[2] CMS Collaboration, "Transverse-momentum and pseudorapidity distributions of charged hadrons in $pp$ collisions at $\sqrt{s}$= 7 TeV", *Phys. Rev. Lett.* **105** (2010) 022002, arXiv:1005.3299. doi:10.1103/PhysRevLett.105.022002.

[3] ALICE Collaboration, "Strange particle production in proton-proton collisions at $\sqrt{s}$ = 0.9 TeV with ALICE at the LHC", arXiv:1012.3257.

[4] LHCb Collaboration, "Prompt $K^0_S$ production in $pp$ collisions at $\sqrt{s} = 0.9$ TeV", *Phys. Lett.* **B693** (2010) 69, arXiv:1008.3105. doi:10.1016/j.physletb.2010.08.055.

[5] T. Sjöstrand, S. Mrenna and P. Skands, "PYTHIA 6.4 physics and manual", *JHEP* **05** (2006) 026. doi:10.1088/1126-6708/2006/05/026.

[6] V. T. Pop, M. Gyulassy, J. Barrette et al., "Strong longitudinal color-field effects in $pp$ collisions at energies available at the CERN Large Hadron Collider", arXiv:1010.5439.

[7] P. Koch, B. Müller, and J. Rafelski, "Strangeness in Relativistic Heavy Ion Collisions", *Phys. Rept.* **142** (1986) 167. doi:10.1016/0370-1573(86)90096-7.

[8] N. Armesto, (ed. ) et al., "Heavy-ion collisions at the LHC – Last Call for Predictions", *J. Phys.* **G35** (2008) 054001, arXiv:0711.0974. doi:10.1088/0954-3899/35/5/054001.

[9] K. Werner, I. Karpenko, and T. Pierog, "Collective effects in proton proton and heavy ion scattering, and the "ridge" at RHIC", *J. Phys. Conf. Ser.* **230** (2010) 012026. doi:10.1088/1742-6596/230/1/012026.

[10] A. K. Likhoded, A. V. Luchinsky, and A. A. Novoselov, "Inclusive light hadron production in $pp$ scattering at the LHC", *Phys. Rev.* **D82** (2010) 114006, arXiv:1005.1827. doi:10.1103/PhysRevD.82.114006.

[11] P. V. Chliapnikov, A. K. Likhoded, and V. A. Uvarov, "Inclusive Cross Sections in the Central Region and the Supercritical Pomeron", *Phys. Lett.* **B215** (1988) 417. doi:10.1016/0370-2693(88)91458-X.

[12] CMS Collaboration, "The CMS experiment at the CERN LHC", *JINST* **3** (2008) S08004. doi:10.1088/1748-0221/3/08/S08004.

[13] P. Bartalini, (ed. ) et al., "Proceedings of the First International Workshop on Multiple Partonic Interactions at the LHC (MPI08)", arXiv:1003.4220.

[14] GEANT4 Collaboration, "GEANT4 – a simulation toolkit", *Nucl. Instrum. Meth.* **A506** (2003) 250. doi:10.1016/S0168-9002(03)01368-8.

[15] CMS Collaboration, "CMS Tracking Performance Results from early LHC Operation", *Eur. Phys. J.* **C70** (2010) 1165, arXiv:1007.1988. doi:10.1140/epjc/s10052-010-1491-3.

[16] Particle Data Group Collaboration, "Review of particle physics", *J. Phys.* **G37** (2010) 075021. doi:10.1088/0954-3899/37/7A/075021.

[17] P. Z. Skands, "The Perugia Tunes", arXiv:0905.3418.

[18] T. Sjöstrand, S. Mrenna and P. Skands, "A Brief Introduction to PYTHIA 8.1", *Comput. Phys. Commun.* **178** (2008) 852, arXiv:0710.3820. doi:10.1016/j.cpc.2008.01.036.

[19] ALICE Collaboration, "Midrapidity antiproton-to-proton ratio in pp collisions at $\sqrt{s} = 0.9$ and 7 TeV measured by the ALICE experiment", *Phys. Rev. Lett.* **105** (2010) 072002, arXiv:1006.5432. doi:10.1103/PhysRevLett.105.072002.

[20] UA5 Collaboration, "Diffraction dissociation at the CERN pulsed $pp$ collider at c.m. Energies of 900 and 200 GeV", *Z. Phys.* **C33** (1986) 175. doi:10.1007/BF01411134.

[21] R. Engel, J. Ranft, and S. Roesler, "Hard diffraction in hadron hadron interactions and in photoproduction", *Phys. Rev.* **D52** (1995) 1459, arXiv:hep-ph/9502319. doi:10.1103/PhysRevD.52.1459.

[22] F. W. Bopp, R. Engel, and J. Ranft, "Rapidity gaps and the PHOJET Monte Carlo", arXiv:hep-ph/9803437.

[23] C. Tsallis, "Possible Generalization of Boltzmann-Gibbs Statistics", *J. Stat. Phys.* **52** (1988) 479. doi:10.1007/BF01016429.

[24] STAR Collaboration, "Strange particle production in $p + p$ collisions at $\sqrt{s} = 200$ GeV", *Phys. Rev.* **C75** (2007) 064901, arXiv:nucl-ex/0607033. doi:10.1103/PhysRevC.75.064901.

[25] CDF Collaboration, "Production of $\Lambda^0$, $\overline{\Lambda}^0$, $\Xi^\pm$, and $\Omega^\pm$ Hyperons in $p\bar{p}$ Collisions at $\sqrt{s} = 1.96$ TeV", arXiv:1101.2996.

[26] CDF Collaboration, "$K^0_S$ and $\Lambda^0$ production studies in $p\bar{p}$ collisions at $\sqrt{s} = 1800$ and 630 GeV", *Phys. Rev.* **D72** (2005) 052001, arXiv:hep-ex/0504048. doi:10.1103/PhysRevD.72.052001.

[27] UA5 Collaboration, "Hyperon Production at 200 and 900 GeV C.M. Energy", *Nucl. Phys.* **B328** (1989) 36. doi:10.1016/0550-3213(89)90090-4.

[28] UA5 Collaboration, "UA5: A general study of proton-antiproton physics at $\sqrt{s}$ = 546 GeV", *Phys. Rept.* **154** (1987) 247. doi:10.1016/0370-1573(87)90130-X.

[29] UA5 Collaboration, "Kaon production in $\bar{p}p$ interactions at c.m. energies from 200 to 900 GeV", *Z. Phys.* **C41** (1988) 179. doi:10.1007/BF01566915.

[30] UA5 Collaboration, "Kaon production in $\bar{p}p$ reactions at a centre-of-mass energy of 540 GeV", *Nucl. Phys.* **B258** (1985) 505. doi:10.1016/0550-3213(85)90624-8.

[31] UA5 Collaboration, "Observation of $\Xi^-$ Production in $p\bar{p}$ Interactions at 540 GeV CMS Energy", *Phys. Lett.* **B151** (1985) 309. doi:10.1016/0370-2693(85)90859-7.

[32] E735 Collaboration, "Hyperon production from $p\bar{p}$ collisions at $\sqrt{s}$ = 1.8 TeV", *Phys. Rev.* **D46** (1992) 2773. doi:10.1103/PhysRevD.46.2773.

[33] CDF Collaboration, "$K^0_S$ production in $\bar{p}p$ interactions at $\sqrt{s} = 630$ GeV and 1800 GeV", *Phys. Rev.* **D40** (1989) 3791. doi:10.1103/PhysRevD.40.3791.

# A The CMS Collaboration

**Yerevan Physics Institute, Yerevan, Armenia**
V. Khachatryan, A.M. Sirunyan, A. Tumasyan

**Institut für Hochenergiephysik der OeAW, Wien, Austria**
W. Adam, T. Bergauer, M. Dragicevic, J. Erö, C. Fabjan, M. Friedl, R. Frühwirth, V.M. Ghete, J. Hammer[1], S. Hänsel, C. Hartl, M. Hoch, N. Hörmann, J. Hrubec, M. Jeitler, G. Kasieczka, W. Kiesenhofer, M. Krammer, D. Liko, I. Mikulec, M. Pernicka, H. Rohringer, R. Schöfbeck, J. Strauss, A. Taurok, F. Teischinger, P. Wagner, W. Waltenberger, G. Walzel, E. Widl, C.-E. Wulz

**National Centre for Particle and High Energy Physics, Minsk, Belarus**
V. Mossolov, N. Shumeiko, J. Suarez Gonzalez

**Universiteit Antwerpen, Antwerpen, Belgium**
L. Benucci, K. Cerny, E.A. De Wolf, X. Janssen, T. Maes, L. Mucibello, S. Ochesanu, B. Roland, R. Rougny, M. Selvaggi, H. Van Haevermaet, P. Van Mechelen, N. Van Remortel

**Vrije Universiteit Brussel, Brussel, Belgium**
S. Beauceron, F. Blekman, S. Blyweert, J. D'Hondt, O. Devroede, R. Gonzalez Suarez, A. Kalogeropoulos, J. Maes, M. Maes, S. Tavernier, W. Van Doninck, P. Van Mulders, G.P. Van Onsem, I. Villella

**Université Libre de Bruxelles, Bruxelles, Belgium**
O. Charaf, B. Clerbaux, G. De Lentdecker, V. Dero, A.P.R. Gay, G.H. Hammad, T. Hreus, P.E. Marage, L. Thomas, C. Vander Velde, P. Vanlaer, J. Wickens

**Ghent University, Ghent, Belgium**
V. Adler, S. Costantini, M. Grunewald, B. Klein, A. Marinov, J. Mccartin, D. Ryckbosch, F. Thyssen, M. Tytgat, L. Vanelderen, P. Verwilligen, S. Walsh, N. Zaganidis

**Université Catholique de Louvain, Louvain-la-Neuve, Belgium**
S. Basegmez, G. Bruno, J. Caudron, L. Ceard, J. De Favereau De Jeneret, C. Delaere, P. Demin, D. Favart, A. Giammanco, G. Grégoire, J. Hollar, V. Lemaitre, J. Liao, O. Militaru, S. Ovyn, D. Pagano, A. Pin, K. Piotrzkowski, N. Schul

**Université de Mons, Mons, Belgium**
N. Beliy, T. Caebergs, E. Daubie

**Centro Brasileiro de Pesquisas Fisicas, Rio de Janeiro, Brazil**
G.A. Alves, D. De Jesus Damiao, M.E. Pol, M.H.G. Souza

**Universidade do Estado do Rio de Janeiro, Rio de Janeiro, Brazil**
W. Carvalho, E.M. Da Costa, C. De Oliveira Martins, S. Fonseca De Souza, L. Mundim, H. Nogima, V. Oguri, W.L. Prado Da Silva, A. Santoro, S.M. Silva Do Amaral, A. Sznajder, F. Torres Da Silva De Araujo

**Instituto de Fisica Teorica, Universidade Estadual Paulista, Sao Paulo, Brazil**
F.A. Dias, M.A.F. Dias, T.R. Fernandez Perez Tomei, E. M. Gregores[2], F. Marinho, S.F. Novaes, Sandra S. Padula

**Institute for Nuclear Research and Nuclear Energy, Sofia, Bulgaria**
N. Darmenov[1], L. Dimitrov, V. Genchev[1], P. Iaydjiev[1], S. Piperov, M. Rodozov, S. Stoykova, G. Sultanov, V. Tcholakov, R. Trayanov, I. Vankov

**University of Sofia, Sofia, Bulgaria**
M. Dyulendarova, R. Hadjiiska, V. Kozhuharov, L. Litov, E. Marinova, M. Mateev, B. Pavlov, P. Petkov

**Institute of High Energy Physics, Beijing, China**
J.G. Bian, G.M. Chen, H.S. Chen, C.H. Jiang, D. Liang, S. Liang, J. Wang, J. Wang, X. Wang, Z. Wang, M. Xu, M. Yang, J. Zang, Z. Zhang

**State Key Lab. of Nucl. Phys. and Tech., Peking University, Beijing, China**
Y. Ban, S. Guo, Y. Guo, W. Li, Y. Mao, S.J. Qian, H. Teng, L. Zhang, B. Zhu, W. Zou

**Universidad de Los Andes, Bogota, Colombia**
A. Cabrera, B. Gomez Moreno, A.A. Ocampo Rios, A.F. Osorio Oliveros, J.C. Sanabria

**Technical University of Split, Split, Croatia**
N. Godinovic, D. Lelas, K. Lelas, R. Plestina[3], D. Polic, I. Puljak

**University of Split, Split, Croatia**
Z. Antunovic, M. Dzelalija

**Institute Rudjer Boskovic, Zagreb, Croatia**
V. Brigljevic, S. Duric, K. Kadija, S. Morovic

**University of Cyprus, Nicosia, Cyprus**
A. Attikis, M. Galanti, J. Mousa, C. Nicolaou, F. Ptochos, P.A. Razis, H. Rykaczewski

**Charles University, Prague, Czech Republic**
M. Finger, M. Finger Jr.

**Academy of Scientific Research and Technology of the Arab Republic of Egypt, Egyptian Network of High Energy Physics, Cairo, Egypt**
Y. Assran[4], M.A. Mahmoud[5]

**National Institute of Chemical Physics and Biophysics, Tallinn, Estonia**
A. Hektor, M. Kadastik, K. Kannike, M. Müntel, M. Raidal, L. Rebane

**Department of Physics, University of Helsinki, Helsinki, Finland**
V. Azzolini, P. Eerola

**Helsinki Institute of Physics, Helsinki, Finland**
S. Czellar, J. Härkönen, A. Heikkinen, V. Karimäki, R. Kinnunen, J. Klem, M.J. Kortelainen, T. Lampén, K. Lassila-Perini, S. Lehti, T. Lindén, P. Luukka, T. Mäenpää, E. Tuominen, J. Tuominiemi, E. Tuovinen, D. Ungaro, L. Wendland

**Lappeenranta University of Technology, Lappeenranta, Finland**
K. Banzuzi, A. Korpela, T. Tuuva

**Laboratoire d'Annecy-le-Vieux de Physique des Particules, IN2P3-CNRS, Annecy-le-Vieux, France**
D. Sillou

**DSM/IRFU, CEA/Saclay, Gif-sur-Yvette, France**
M. Besancon, S. Choudhury, M. Dejardin, D. Denegri, B. Fabbro, J.L. Faure, F. Ferri, S. Ganjour, F.X. Gentit, A. Givernaud, P. Gras, G. Hamel de Monchenault, P. Jarry, E. Locci, J. Malcles, M. Marionneau, L. Millischer, J. Rander, A. Rosowsky, I. Shreyber, M. Titov, P. Verrecchia

**Laboratoire Leprince-Ringuet, Ecole Polytechnique, IN2P3-CNRS, Palaiseau, France**
S. Baffioni, F. Beaudette, L. Bianchini, M. Bluj[6], C. Broutin, P. Busson, C. Charlot, T. Dahms, L. Dobrzynski, R. Granier de Cassagnac, M. Haguenauer, P. Miné, C. Mironov, C. Ochando, P. Paganini, D. Sabes, R. Salerno, Y. Sirois, C. Thiebaux, B. Wyslouch[7], A. Zabi

**Institut Pluridisciplinaire Hubert Curien, Université de Strasbourg, Université de Haute Alsace Mulhouse, CNRS/IN2P3, Strasbourg, France**
J.-L. Agram[8], J. Andrea, A. Besson, D. Bloch, D. Bodin, J.-M. Brom, M. Cardaci, E.C. Chabert, C. Collard, E. Conte[8], F. Drouhin[8], C. Ferro, J.-C. Fontaine[8], D. Gelé, U. Goerlach, S. Greder, P. Juillot, M. Karim[8], A.-C. Le Bihan, Y. Mikami, P. Van Hove

**Centre de Calcul de l'Institut National de Physique Nucleaire et de Physique des Particules (IN2P3), Villeurbanne, France**
F. Fassi, D. Mercier

**Université de Lyon, Université Claude Bernard Lyon 1, CNRS-IN2P3, Institut de Physique Nucléaire de Lyon, Villeurbanne, France**
C. Baty, N. Beaupere, M. Bedjidian, O. Bondu, G. Boudoul, D. Boumediene, H. Brun, N. Chanon, R. Chierici, D. Contardo, P. Depasse, H. El Mamouni, A. Falkiewicz, J. Fay, S. Gascon, B. Ille, T. Kurca, T. Le Grand, M. Lethuillier, L. Mirabito, S. Perries, V. Sordini, S. Tosi, Y. Tschudi, P. Verdier, H. Xiao

**E. Andronikashvili Institute of Physics, Academy of Science, Tbilisi, Georgia**
L. Megrelidze, V. Roinishvili

**Institute of High Energy Physics and Informatization, Tbilisi State University, Tbilisi, Georgia**
D. Lomidze

**RWTH Aachen University, I. Physikalisches Institut, Aachen, Germany**
G. Anagnostou, M. Edelhoff, L. Feld, N. Heracleous, O. Hindrichs, R. Jussen, K. Klein, J. Merz, N. Mohr, A. Ostapchuk, A. Perieanu, F. Raupach, J. Sammet, S. Schael, D. Sprenger, H. Weber, M. Weber, B. Wittmer

**RWTH Aachen University, III. Physikalisches Institut A, Aachen, Germany**
M. Ata, W. Bender, M. Erdmann, J. Frangenheim, T. Hebbeker, A. Hinzmann, K. Hoepfner, C. Hof, T. Klimkovich, D. Klingebiel, P. Kreuzer, D. Lanske[†], C. Magass, G. Masetti, M. Merschmeyer, A. Meyer, P. Papacz, H. Pieta, H. Reithler, S.A. Schmitz, L. Sonnenschein, J. Steggemann, D. Teyssier

**RWTH Aachen University, III. Physikalisches Institut B, Aachen, Germany**
M. Bontenackels, M. Davids, M. Duda, G. Flügge, H. Geenen, M. Giffels, W. Haj Ahmad, D. Heydhausen, T. Kress, Y. Kuessel, A. Linn, A. Nowack, L. Perchalla, O. Pooth, J. Rennefeld, P. Sauerland, A. Stahl, M. Thomas, D. Tornier, M.H. Zoeller

**Deutsches Elektronen-Synchrotron, Hamburg, Germany**
M. Aldaya Martin, W. Behrenhoff, U. Behrens, M. Bergholz[9], K. Borras, A. Cakir, A. Campbell, E. Castro, D. Dammann, G. Eckerlin, D. Eckstein, A. Flossdorf, G. Flucke, A. Geiser, I. Glushkov, J. Hauk, H. Jung, M. Kasemann, I. Katkov, P. Katsas, C. Kleinwort, H. Kluge, A. Knutsson, D. Krücker, E. Kuznetsova, W. Lange, W. Lohmann[9], R. Mankel, M. Marienfeld, I.-A. Melzer-Pellmann, A.B. Meyer, J. Mnich, A. Mussgiller, J. Olzem, A. Parenti, A. Raspereza, A. Raval, R. Schmidt[9], T. Schoerner-Sadenius, N. Sen, M. Stein, J. Tomaszewska, D. Volyanskyy, R. Walsh, C. Wissing

**University of Hamburg, Hamburg, Germany**
C. Autermann, S. Bobrovskyi, J. Draeger, H. Enderle, U. Gebbert, K. Kaschube, G. Kaussen, R. Klanner, J. Lange, B. Mura, S. Naumann-Emme, F. Nowak, N. Pietsch, C. Sander, H. Schettler, P. Schleper, M. Schröder, T. Schum, J. Schwandt, A.K. Srivastava, H. Stadie, G. Steinbrück, J. Thomsen, R. Wolf

**Institut für Experimentelle Kernphysik, Karlsruhe, Germany**
C. Barth, J. Bauer, V. Buege, T. Chwalek, W. De Boer, A. Dierlamm, G. Dirkes, M. Feindt, J. Gruschke, C. Hackstein, F. Hartmann, S.M. Heindl, M. Heinrich, H. Held, K.H. Hoffmann, S. Honc, T. Kuhr, D. Martschei, S. Mueller, Th. Müller, M. Niegel, O. Oberst, A. Oehler, J. Ott, T. Peiffer, D. Piparo, G. Quast, K. Rabbertz, F. Ratnikov, M. Renz, C. Saout, A. Scheurer, P. Schieferdecker, F.-P. Schilling, G. Schott, H.J. Simonis, F.M. Stober, D. Troendle, J. Wagner-Kuhr, M. Zeise, V. Zhukov[10], E.B. Ziebarth

**Institute of Nuclear Physics "Demokritos", Aghia Paraskevi, Greece**
G. Daskalakis, T. Geralis, S. Kesisoglou, A. Kyriakis, D. Loukas, I. Manolakos, A. Markou, C. Markou, C. Mavrommatis, E. Ntomari, E. Petrakou

**University of Athens, Athens, Greece**
L. Gouskos, T.J. Mertzimekis, A. Panagiotou

**University of Ioánnina, Ioánnina, Greece**
I. Evangelou, C. Foudas, P. Kokkas, N. Manthos, I. Papadopoulos, V. Patras, F.A. Triantis

**KFKI Research Institute for Particle and Nuclear Physics, Budapest, Hungary**
A. Aranyi, G. Bencze, L. Boldizsar, G. Debreczeni, C. Hajdu[1], D. Horvath[11], A. Kapusi, K. Krajczar[12], A. Laszlo, F. Sikler, G. Vesztergombi[12]

**Institute of Nuclear Research ATOMKI, Debrecen, Hungary**
N. Beni, J. Molnar, J. Palinkas, Z. Szillasi, V. Veszpremi

**University of Debrecen, Debrecen, Hungary**
P. Raics, Z.L. Trocsanyi, B. Ujvari

**Panjab University, Chandigarh, India**
S. Bansal, S.B. Beri, V. Bhatnagar, N. Dhingra, R. Gupta, M. Jindal, M. Kaur, J.M. Kohli, M.Z. Mehta, N. Nishu, L.K. Saini, A. Sharma, A.P. Singh, J.B. Singh, S.P. Singh

**University of Delhi, Delhi, India**
S. Ahuja, S. Bhattacharya, B.C. Choudhary, P. Gupta, S. Jain, S. Jain, A. Kumar, R.K. Shivpuri

**Bhabha Atomic Research Centre, Mumbai, India**
R.K. Choudhury, D. Dutta, S. Kailas, S.K. Kataria, A.K. Mohanty[1], L.M. Pant, P. Shukla

**Tata Institute of Fundamental Research - EHEP, Mumbai, India**
T. Aziz, M. Guchait[13], A. Gurtu, M. Maity[14], D. Majumder, G. Majumder, K. Mazumdar, G.B. Mohanty, A. Saha, K. Sudhakar, N. Wickramage

**Tata Institute of Fundamental Research - HECR, Mumbai, India**
S. Banerjee, S. Dugad, N.K. Mondal

**Institute for Research and Fundamental Sciences (IPM), Tehran, Iran**
H. Arfaei, H. Bakhshiansohi, S.M. Etesami, A. Fahim, M. Hashemi, A. Jafari, M. Khakzad, A. Mohammadi, M. Mohammadi Najafabadi, S. Paktinat Mehdiabadi, B. Safarzadeh, M. Zeinali

**INFN Sezione di Bari [a], Università di Bari [b], Politecnico di Bari [c], Bari, Italy**
M. Abbrescia[a,b], L. Barbone[a,b], C. Calabria[a,b], A. Colaleo[a], D. Creanza[a,c], N. De Filippis[a,c], M. De Palma[a,b], A. Dimitrov[a], L. Fiore[a], G. Iaselli[a,c], L. Lusito[a,b,1], G. Maggi[a,c], M. Maggi[a], N. Manna[a,b], B. Marangelli[a,b], S. My[a,c], S. Nuzzo[a,b], N. Pacifico[a,b], G.A. Pierro[a], A. Pompili[a,b], G. Pugliese[a,c], F. Romano[a,c], G. Roselli[a,b], G. Selvaggi[a,b], L. Silvestris[a], R. Trentadue[a], S. Tupputi[a,b], G. Zito[a]

**INFN Sezione di Bologna [a], Università di Bologna [b], Bologna, Italy**
G. Abbiendi[a], A.C. Benvenuti[a], D. Bonacorsi[a], S. Braibant-Giacomelli[a,b], L. Brigliadori[a], P. Capiluppi[a,b], A. Castro[a,b], F.R. Cavallo[a], M. Cuffiani[a,b], G.M. Dallavalle[a], F. Fabbri[a], A. Fanfani[a,b], D. Fasanella[a], P. Giacomelli[a], M. Giunta[a], C. Grandi[a], S. Marcellini[a], M. Meneghelli[a,b], A. Montanari[a], F.L. Navarria[a,b], F. Odorici[a], A. Perrotta[a], F. Primavera[a], A.M. Rossi[a,b], T. Rovelli[a,b], G. Siroli[a,b], R. Travaglini[a,b]

**INFN Sezione di Catania [a], Università di Catania [b], Catania, Italy**
S. Albergo[a,b], G. Cappello[a,b], M. Chiorboli[a,b,1], S. Costa[a,b], A. Tricomi[a,b], C. Tuve[a]

**INFN Sezione di Firenze [a], Università di Firenze [b], Firenze, Italy**
G. Barbagli[a], V. Ciulli[a,b], C. Civinini[a], R. D'Alessandro[a,b], E. Focardi[a,b], S. Frosali[a,b], E. Gallo[a], S. Gonzi[a,b], P. Lenzi[a,b], M. Meschini[a], S. Paoletti[a], G. Sguazzoni[a], A. Tropiano[a,1]

**INFN Laboratori Nazionali di Frascati, Frascati, Italy**
L. Benussi, S. Bianco, S. Colafranceschi[15], F. Fabbri, D. Piccolo

**INFN Sezione di Genova, Genova, Italy**
P. Fabbricatore, R. Musenich

**INFN Sezione di Milano-Biccoca [a], Università di Milano-Bicocca [b], Milano, Italy**
A. Benaglia[a,b], F. De Guio[a,b,1], L. Di Matteo[a,b], A. Ghezzi[a,b,1], M. Malberti[a,b], S. Malvezzi[a], A. Martelli[a,b], A. Massironi[a,b], D. Menasce[a], L. Moroni[a], M. Paganoni[a,b], D. Pedrini[a], S. Ragazzi[a,b], N. Redaelli[a], S. Sala[a], T. Tabarelli de Fatis[a,b], V. Tancini[a,b]

**INFN Sezione di Napoli [a], Università di Napoli "Federico II" [b], Napoli, Italy**
S. Buontempo[a], C.A. Carrillo Montoya[a], A. Cimmino[a,b], A. De Cosa[a,b], M. De Gruttola[a,b], F. Fabozzi[a,16], A.O.M. Iorio[a], L. Lista[a], M. Merola[a,b], P. Noli[a,b], P. Paolucci[a]

**INFN Sezione di Padova [a], Università di Padova [b], Università di Trento (Trento) [c], Padova, Italy**
P. Azzi[a], N. Bacchetta[a], P. Bellan[a,b], M. Biasotto[a,17], D. Bisello[a,b], A. Branca[a], R. Carlin[a,b], P. Checchia[a], E. Conti[a], M. De Mattia[a,b], T. Dorigo[a], U. Dosselli[a], F. Fanzago[a], F. Gasparini[a,b], P. Giubilato[a,b], A. Gresele[a,c], S. Lacaprara[a,17], I. Lazzizzera[a,c], M. Margoni[a,b], A.T. Meneguzzo[a,b], M. Nespolo[a,1], L. Perrozzi[a,1], N. Pozzobon[a,b], P. Ronchese[a,b], F. Simonetto[a,b], E. Torassa[a], M. Tosi[a,b], S. Vanini[a,b], P. Zotto[a,b], G. Zumerle[a,b]

**INFN Sezione di Pavia [a], Università di Pavia [b], Pavia, Italy**
U. Berzano[a], C. Riccardi[a,b], P. Torre[a,b], P. Vitulo[a,b]

**INFN Sezione di Perugia [a], Università di Perugia [b], Perugia, Italy**
M. Biasini[a,b], G.M. Bilei[a], B. Caponeri[a,b], L. Fanò[a,b], P. Lariccia[a,b], A. Lucaroni[a,b,1], G. Mantovani[a,b], M. Menichelli[a], A. Nappi[a,b], A. Santocchia[a,b], L. Servoli[a], S. Taroni[a,b], M. Valdata[a,b], R. Volpe[a,b,1]

**INFN Sezione di Pisa [a], Università di Pisa [b], Scuola Normale Superiore di Pisa [c], Pisa, Italy**
P. Azzurri[a,c], G. Bagliesi[a], J. Bernardini[a,b], T. Boccali[a,1], G. Broccolo[a,c], R. Castaldi[a], R.T. D'Agnolo[a,c], R. Dell'Orso[a], F. Fiori[a,b], L. Foà[a,c], A. Giassi[a], A. Kraan[a], F. Ligabue[a,c],

T. Lomtadze[a], L. Martini[a,18], A. Messineo[a,b], F. Palla[a], F. Palmonari[a], S. Sarkar[a,c], G. Segneri[a], A.T. Serban[a], P. Spagnolo[a], R. Tenchini[a], G. Tonelli[a,b,1], A. Venturi[a,1], P.G. Verdini[a]

**INFN Sezione di Roma [a], Università di Roma "La Sapienza" [b], Roma, Italy**
L. Barone[a,b], F. Cavallari[a], D. Del Re[a,b], E. Di Marco[a,b], M. Diemoz[a], D. Franci[a,b], M. Grassi[a], E. Longo[a,b], S. Nourbakhsh[a], G. Organtini[a,b], A. Palma[a,b], F. Pandolfi[a,b,1], R. Paramatti[a], S. Rahatlou[a,b]

**INFN Sezione di Torino [a], Università di Torino [b], Università del Piemonte Orientale (Novara) [c], Torino, Italy**
N. Amapane[a,b], R. Arcidiacono[a,c], S. Argiro[a,b], M. Arneodo[a,c], C. Biino[a], C. Botta[a,b,1], N. Cartiglia[a], R. Castello[a,b], M. Costa[a,b], N. Demaria[a], A. Graziano[a,b,1], C. Mariotti[a], M. Marone[a,b], S. Maselli[a], E. Migliore[a,b], G. Mila[a,b], V. Monaco[a,b], M. Musich[a,b], M.M. Obertino[a,c], N. Pastrone[a], M. Pelliccioni[a,b,1], A. Romero[a,b], M. Ruspa[a,c], R. Sacchi[a,b], V. Sola[a,b], A. Solano[a,b], A. Staiano[a], D. Trocino[a,b], A. Vilela Pereira[a,b,1]

**INFN Sezione di Trieste [a], Università di Trieste [b], Trieste, Italy**
S. Belforte[a], F. Cossutti[a], G. Della Ricca[a,b], B. Gobbo[a], D. Montanino[a,b], A. Penzo[a]

**Kangwon National University, Chunchon, Korea**
S.G. Heo

**Kyungpook National University, Daegu, Korea**
S. Chang, J. Chung, D.H. Kim, G.N. Kim, J.E. Kim, D.J. Kong, H. Park, D. Son, D.C. Son

**Chonnam National University, Institute for Universe and Elementary Particles, Kwangju, Korea**
Zero Kim, J.Y. Kim, S. Song

**Korea University, Seoul, Korea**
S. Choi, B. Hong, M. Jo, H. Kim, J.H. Kim, T.J. Kim, K.S. Lee, D.H. Moon, S.K. Park, H.B. Rhee, E. Seo, S. Shin, K.S. Sim

**University of Seoul, Seoul, Korea**
M. Choi, S. Kang, H. Kim, C. Park, I.C. Park, S. Park, G. Ryu

**Sungkyunkwan University, Suwon, Korea**
Y. Choi, Y.K. Choi, J. Goh, J. Lee, S. Lee, H. Seo, I. Yu

**Vilnius University, Vilnius, Lithuania**
M.J. Bilinskas, I. Grigelionis, M. Janulis, D. Martisiute, P. Petrov, T. Sabonis

**Centro de Investigacion y de Estudios Avanzados del IPN, Mexico City, Mexico**
H. Castilla-Valdez, E. De La Cruz-Burelo, R. Lopez-Fernandez, A. Sánchez-Hernández, L.M. Villasenor-Cendejas

**Universidad Iberoamericana, Mexico City, Mexico**
S. Carrillo Moreno, F. Vazquez Valencia

**Benemerita Universidad Autonoma de Puebla, Puebla, Mexico**
H.A. Salazar Ibarguen

**Universidad Autónoma de San Luis Potosí, San Luis Potosí, Mexico**
E. Casimiro Linares, A. Morelos Pineda, M.A. Reyes-Santos

**University of Auckland, Auckland, New Zealand**
P. Allfrey, D. Krofcheck

**University of Canterbury, Christchurch, New Zealand**
P.H. Butler, R. Doesburg, H. Silverwood

**National Centre for Physics, Quaid-I-Azam University, Islamabad, Pakistan**
M. Ahmad, I. Ahmed, M.I. Asghar, H.R. Hoorani, W.A. Khan, T. Khurshid, S. Qazi

**Institute of Experimental Physics, Faculty of Physics, University of Warsaw, Warsaw, Poland**
M. Cwiok, W. Dominik, K. Doroba, A. Kalinowski, M. Konecki, J. Krolikowski

**Soltan Institute for Nuclear Studies, Warsaw, Poland**
T. Frueboes, R. Gokieli, M. Górski, M. Kazana, K. Nawrocki, K. Romanowska-Rybinska, M. Szleper, G. Wrochna, P. Zalewski

**Laboratório de Instrumentação e Física Experimental de Partículas, Lisboa, Portugal**
N. Almeida, A. David, P. Faccioli, P.G. Ferreira Parracho, M. Gallinaro, P. Martins, P. Musella, A. Nayak, P.Q. Ribeiro, J. Seixas, P. Silva, J. Varela, H.K. Wöhri

**Joint Institute for Nuclear Research, Dubna, Russia**
I. Belotelov, P. Bunin, I. Golutvin, A. Kamenev, V. Karjavin, G. Kozlov, A. Lanev, P. Moisenz, V. Palichik, V. Perelygin, S. Shmatov, V. Smirnov, A. Volodko, A. Zarubin

**Petersburg Nuclear Physics Institute, Gatchina (St Petersburg), Russia**
N. Bondar, V. Golovtsov, Y. Ivanov, V. Kim, P. Levchenko, V. Murzin, V. Oreshkin, I. Smirnov, V. Sulimov, L. Uvarov, S. Vavilov, A. Vorobyev

**Institute for Nuclear Research, Moscow, Russia**
Yu. Andreev, S. Gninenko, N. Golubev, M. Kirsanov, N. Krasnikov, V. Matveev, A. Pashenkov, A. Toropin, S. Troitsky

**Institute for Theoretical and Experimental Physics, Moscow, Russia**
V. Epshteyn, V. Gavrilov, V. Kaftanov[†], M. Kossov[1], A. Krokhotin, N. Lychkovskaya, G. Safronov, S. Semenov, V. Stolin, E. Vlasov, A. Zhokin

**Moscow State University, Moscow, Russia**
E. Boos, M. Dubinin[19], L. Dudko, A. Ershov, A. Gribushin, O. Kodolova, I. Lokhtin, S. Obraztsov, S. Petrushanko, L. Sarycheva, V. Savrin, A. Snigirev

**P.N. Lebedev Physical Institute, Moscow, Russia**
V. Andreev, M. Azarkin, I. Dremin, M. Kirakosyan, S.V. Rusakov, A. Vinogradov

**State Research Center of Russian Federation, Institute for High Energy Physics, Protvino, Russia**
I. Azhgirey, S. Bitioukov, V. Grishin[1], V. Kachanov, D. Konstantinov, A. Korablev, V. Krychkine, V. Petrov, R. Ryutin, S. Slabospitsky, A. Sobol, L. Tourtchanovitch, S. Troshin, N. Tyurin, A. Uzunian, A. Volkov

**University of Belgrade, Faculty of Physics and Vinca Institute of Nuclear Sciences, Belgrade, Serbia**
P. Adzic[20], M. Djordjevic, D. Krpic[20], J. Milosevic

**Centro de Investigaciones Energéticas Medioambientales y Tecnológicas (CIEMAT), Madrid, Spain**
M. Aguilar-Benitez, J. Alcaraz Maestre, P. Arce, C. Battilana, E. Calvo, M. Cepeda, M. Cerrada, N. Colino, B. De La Cruz, C. Diez Pardos, D. Domínguez Vázquez, C. Fernandez Bedoya, J.P. Fernández Ramos, A. Ferrando, J. Flix, M.C. Fouz, P. Garcia-Abia, O. Gonzalez Lopez,

S. Goy Lopez, J.M. Hernandez, M.I. Josa, G. Merino, J. Puerta Pelayo, I. Redondo, L. Romero, J. Santaolalla, C. Willmott

**Universidad Autónoma de Madrid, Madrid, Spain**
C. Albajar, G. Codispoti, J.F. de Trocóniz

**Universidad de Oviedo, Oviedo, Spain**
J. Cuevas, J. Fernandez Menendez, S. Folgueras, I. Gonzalez Caballero, L. Lloret Iglesias, J.M. Vizan Garcia

**Instituto de Física de Cantabria (IFCA), CSIC-Universidad de Cantabria, Santander, Spain**
J.A. Brochero Cifuentes, I.J. Cabrillo, A. Calderon, M. Chamizo Llatas, S.H. Chuang, J. Duarte Campderros, M. Felcini[21], M. Fernandez, G. Gomez, J. Gonzalez Sanchez, C. Jorda, P. Lobelle Pardo, A. Lopez Virto, J. Marco, R. Marco, C. Martinez Rivero, F. Matorras, F.J. Munoz Sanchez, J. Piedra Gomez[22], T. Rodrigo, A. Ruiz-Jimeno, L. Scodellaro, M. Sobron Sanudo, I. Vila, R. Vilar Cortabitarte

**CERN, European Organization for Nuclear Research, Geneva, Switzerland**
D. Abbaneo, E. Auffray, G. Auzinger, P. Baillon, A.H. Ball, D. Barney, A.J. Bell[23], D. Benedetti, C. Bernet[3], W. Bialas, P. Bloch, A. Bocci, S. Bolognesi, H. Breuker, G. Brona, K. Bunkowski, T. Camporesi, E. Cano, G. Cerminara, T. Christiansen, J.A. Coarasa Perez, B. Curé, D. D'Enterria, A. De Roeck, S. Di Guida, F. Duarte Ramos, A. Elliott-Peisert, B. Frisch, W. Funk, A. Gaddi, S. Gennai, G. Georgiou, H. Gerwig, D. Gigi, K. Gill, D. Giordano, F. Glege, R. Gomez-Reino Garrido, M. Gouzevitch, P. Govoni, S. Gowdy, L. Guiducci, M. Hansen, J. Harvey, J. Hegeman, B. Hegner, C. Henderson, G. Hesketh, H.F. Hoffmann, A. Honma, V. Innocente, P. Janot, K. Kaadze, E. Karavakis, P. Lecoq, C. Lourenço, A. Macpherson, T. Mäki, L. Malgeri, M. Mannelli, L. Masetti, F. Meijers, S. Mersi, E. Meschi, R. Moser, M.U. Mozer, M. Mulders, E. Nesvold[1], M. Nguyen, T. Orimoto, L. Orsini, E. Perez, A. Petrilli, A. Pfeiffer, M. Pierini, M. Pimiä, G. Polese, A. Racz, J. Rodrigues Antunes, G. Rolandi[24], T. Rommerskirchen, C. Rovelli[25], M. Rovere, H. Sakulin, C. Schäfer, C. Schwick, I. Segoni, A. Sharma, P. Siegrist, M. Simon, P. Sphicas[26], D. Spiga, M. Spiropulu[19], F. Stöckli, M. Stoye, P. Tropea, A. Tsirou, A. Tsyganov, G.I. Veres[12], P. Vichoudis, M. Voutilainen, W.D. Zeuner

**Paul Scherrer Institut, Villigen, Switzerland**
W. Bertl, K. Deiters, W. Erdmann, K. Gabathuler, R. Horisberger, Q. Ingram, H.C. Kaestli, S. König, D. Kotlinski, U. Langenegger, F. Meier, D. Renker, T. Rohe, J. Sibille[27], A. Starodumov[28]

**Institute for Particle Physics, ETH Zurich, Zurich, Switzerland**
P. Bortignon, L. Caminada[29], Z. Chen, S. Cittolin, G. Dissertori, M. Dittmar, J. Eugster, K. Freudenreich, C. Grab, A. Hervé, W. Hintz, P. Lecomte, W. Lustermann, C. Marchica[29], P. Martinez Ruiz del Arbol, P. Meridiani, P. Milenovic[30], F. Moortgat, P. Nef, F. Nessi-Tedaldi, L. Pape, F. Pauss, T. Punz, A. Rizzi, F.J. Ronga, M. Rossini, L. Sala, A.K. Sanchez, M.-C. Sawley, B. Stieger, L. Tauscher[†], A. Thea, K. Theofilatos, D. Treille, C. Urscheler, R. Wallny, M. Weber, L. Wehrli, J. Weng

**Universität Zürich, Zurich, Switzerland**
E. Aguiló, C. Amsler, V. Chiochia, S. De Visscher, C. Favaro, M. Ivova Rikova, B. Millan Mejias, C. Regenfus, P. Robmann, A. Schmidt, H. Snoek

**National Central University, Chung-Li, Taiwan**
Y.H. Chang, K.H. Chen, W.T. Chen, S. Dutta, A. Go, C.M. Kuo, S.W. Li, W. Lin, M.H. Liu, Z.K. Liu, Y.J. Lu, D. Mekterovic, J.H. Wu, S.S. Yu

**National Taiwan University (NTU), Taipei, Taiwan**
P. Bartalini, P. Chang, Y.H. Chang, Y.W. Chang, Y. Chao, K.F. Chen, W.-S. Hou, Y. Hsiung, K.Y. Kao, Y.J. Lei, R.-S. Lu, J.G. Shiu, Y.M. Tzeng, M. Wang

**Cukurova University, Adana, Turkey**
A. Adiguzel, M.N. Bakirci[31], S. Cerci[32], Z. Demir, C. Dozen, I. Dumanoglu, E. Eskut, S. Girgis, G. Gokbulut, Y. Guler, E. Gurpinar, I. Hos, E.E. Kangal, T. Karaman, A. Kayis Topaksu, A. Nart, G. Onengut, K. Ozdemir, S. Ozturk, A. Polatoz, K. Sogut[33], B. Tali, H. Topakli[31], D. Uzun, L.N. Vergili, M. Vergili, C. Zorbilmez

**Middle East Technical University, Physics Department, Ankara, Turkey**
I.V. Akin, T. Aliev, S. Bilmis, M. Deniz, H. Gamsizkan, A.M. Guler, K. Ocalan, A. Ozpineci, M. Serin, R. Sever, U.E. Surat, E. Yildirim, M. Zeyrek

**Bogazici University, Istanbul, Turkey**
M. Deliomeroglu, D. Demir[34], E. Gülmez, A. Halu, B. Isildak, M. Kaya[35], O. Kaya[35], S. Ozkorucuklu[36], N. Sonmez[37]

**National Scientific Center, Kharkov Institute of Physics and Technology, Kharkov, Ukraine**
L. Levchuk

**University of Bristol, Bristol, United Kingdom**
P. Bell, F. Bostock, J.J. Brooke, T.L. Cheng, E. Clement, D. Cussans, R. Frazier, J. Goldstein, M. Grimes, M. Hansen, D. Hartley, G.P. Heath, H.F. Heath, B. Huckvale, J. Jackson, L. Kreczko, S. Metson, D.M. Newbold[38], K. Nirunpong, A. Poll, S. Senkin, V.J. Smith, S. Ward

**Rutherford Appleton Laboratory, Didcot, United Kingdom**
L. Basso[39], K.W. Bell, A. Belyaev[39], C. Brew, R.M. Brown, B. Camanzi, D.J.A. Cockerill, J.A. Coughlan, K. Harder, S. Harper, B.W. Kennedy, E. Olaiya, D. Petyt, B.C. Radburn-Smith, C.H. Shepherd-Themistocleous, I.R. Tomalin, W.J. Womersley, S.D. Worm

**Imperial College, London, United Kingdom**
R. Bainbridge, G. Ball, J. Ballin, R. Beuselinck, O. Buchmuller, D. Colling, N. Cripps, M. Cutajar, G. Davies, M. Della Negra, J. Fulcher, D. Futyan, A. Guneratne Bryer, G. Hall, Z. Hatherell, J. Hays, G. Iles, G. Karapostoli, L. Lyons, A.-M. Magnan, J. Marrouche, R. Nandi, J. Nash, A. Nikitenko[28], A. Papageorgiou, M. Pesaresi, K. Petridis, M. Pioppi[40], D.M. Raymond, N. Rompotis, A. Rose, M.J. Ryan, C. Seez, P. Sharp, A. Sparrow, A. Tapper, S. Tourneur, M. Vazquez Acosta, T. Virdee, S. Wakefield, D. Wardrope, T. Whyntie

**Brunel University, Uxbridge, United Kingdom**
M. Barrett, M. Chadwick, J.E. Cole, P.R. Hobson, A. Khan, P. Kyberd, D. Leslie, W. Martin, I.D. Reid, L. Teodorescu

**Baylor University, Waco, USA**
K. Hatakeyama

**Boston University, Boston, USA**
T. Bose, E. Carrera Jarrin, C. Fantasia, A. Heister, J. St. John, P. Lawson, D. Lazic, J. Rohlf, D. Sperka, L. Sulak

**Brown University, Providence, USA**
A. Avetisyan, S. Bhattacharya, J.P. Chou, D. Cutts, A. Ferapontov, U. Heintz, S. Jabeen, G. Kukartsev, G. Landsberg, M. Narain, D. Nguyen, M. Segala, T. Speer, K.V. Tsang

**University of California, Davis, Davis, USA**
M.A. Borgia, R. Breedon, M. Calderon De La Barca Sanchez, D. Cebra, S. Chauhan, M. Chertok, J. Conway, P.T. Cox, J. Dolen, R. Erbacher, E. Friis, W. Ko, A. Kopecky, R. Lander, H. Liu, S. Maruyama, T. Miceli, M. Nikolic, D. Pellett, J. Robles, S. Salur, T. Schwarz, M. Searle, J. Smith, M. Squires, M. Tripathi, R. Vasquez Sierra, C. Veelken

**University of California, Los Angeles, Los Angeles, USA**
V. Andreev, K. Arisaka, D. Cline, R. Cousins, A. Deisher, J. Duris, S. Erhan, C. Farrell, J. Hauser, M. Ignatenko, C. Jarvis, C. Plager, G. Rakness, P. Schlein[†], J. Tucker, V. Valuev

**University of California, Riverside, Riverside, USA**
J. Babb, R. Clare, J. Ellison, J.W. Gary, F. Giordano, G. Hanson, G.Y. Jeng, S.C. Kao, F. Liu, H. Liu, A. Luthra, H. Nguyen, B.C. Shen[†], R. Stringer, J. Sturdy, S. Sumowidagdo, R. Wilken, S. Wimpenny

**University of California, San Diego, La Jolla, USA**
W. Andrews, J.G. Branson, G.B. Cerati, E. Dusinberre, D. Evans, F. Golf, A. Holzner, R. Kelley, M. Lebourgeois, J. Letts, B. Mangano, J. Muelmenstaedt, S. Padhi, C. Palmer, G. Petrucciani, H. Pi, M. Pieri, R. Ranieri, M. Sani, V. Sharma[1], S. Simon, Y. Tu, A. Vartak, F. Würthwein, A. Yagil

**University of California, Santa Barbara, Santa Barbara, USA**
D. Barge, R. Bellan, C. Campagnari, M. D'Alfonso, T. Danielson, K. Flowers, P. Geffert, J. Incandela, C. Justus, P. Kalavase, S.A. Koay, D. Kovalskyi, V. Krutelyov, S. Lowette, N. Mccoll, V. Pavlunin, F. Rebassoo, J. Ribnik, J. Richman, R. Rossin, D. Stuart, W. To, J.R. Vlimant

**California Institute of Technology, Pasadena, USA**
A. Bornheim, J. Bunn, Y. Chen, M. Gataullin, D. Kcira, V. Litvine, Y. Ma, A. Mott, H.B. Newman, C. Rogan, V. Timciuc, P. Traczyk, J. Veverka, R. Wilkinson, Y. Yang, R.Y. Zhu

**Carnegie Mellon University, Pittsburgh, USA**
B. Akgun, R. Carroll, T. Ferguson, Y. Iiyama, D.W. Jang, S.Y. Jun, Y.F. Liu, M. Paulini, J. Russ, N. Terentyev, H. Vogel, I. Vorobiev

**University of Colorado at Boulder, Boulder, USA**
J.P. Cumalat, M.E. Dinardo, B.R. Drell, C.J. Edelmaier, W.T. Ford, A. Gaz, B. Heyburn, E. Luiggi Lopez, U. Nauenberg, J.G. Smith, K. Stenson, K.A. Ulmer, S.R. Wagner, S.L. Zang

**Cornell University, Ithaca, USA**
L. Agostino, J. Alexander, A. Chatterjee, S. Das, N. Eggert, L.J. Fields, L.K. Gibbons, B. Heltsley, W. Hopkins, A. Khukhunaishvili, B. Kreis, V. Kuznetsov, G. Nicolas Kaufman, J.R. Patterson, D. Puigh, D. Riley, A. Ryd, X. Shi, W. Sun, W.D. Teo, J. Thom, J. Thompson, J. Vaughan, Y. Weng, L. Winstrom, P. Wittich

**Fairfield University, Fairfield, USA**
A. Biselli, G. Cirino, D. Winn

**Fermi National Accelerator Laboratory, Batavia, USA**
S. Abdullin, M. Albrow, J. Anderson, G. Apollinari, M. Atac, J.A. Bakken, S. Banerjee, L.A.T. Bauerdick, A. Beretvas, J. Berryhill, P.C. Bhat, I. Bloch, F. Borcherding, K. Burkett, J.N. Butler, V. Chetluru, H.W.K. Cheung, F. Chlebana, S. Cihangir, M. Demarteau, D.P. Eartly, V.D. Elvira, S. Esen, I. Fisk, J. Freeman, Y. Gao, E. Gottschalk, D. Green, K. Gunthoti, O. Gutsche, A. Hahn, J. Hanlon, R.M. Harris, J. Hirschauer, B. Hooberman, E. James, H. Jensen, M. Johnson, U. Joshi, R. Khatiwada, B. Kilminster, B. Klima, K. Kousouris, S. Kunori, S. Kwan,

C. Leonidopoulos, P. Limon, R. Lipton, J. Lykken, K. Maeshima, J.M. Marraffino, D. Mason, P. McBride, T. McCauley, T. Miao, K. Mishra, S. Mrenna, Y. Musienko[41], C. Newman-Holmes, V. O'Dell, S. Popescu[42], R. Pordes, O. Prokofyev, N. Saoulidou, E. Sexton-Kennedy, S. Sharma, A. Soha, W.J. Spalding, L. Spiegel, P. Tan, L. Taylor, S. Tkaczyk, L. Uplegger, E.W. Vaandering, R. Vidal, J. Whitmore, W. Wu, F. Yang, F. Yumiceva, J.C. Yun

**University of Florida, Gainesville, USA**
D. Acosta, P. Avery, D. Bourilkov, M. Chen, G.P. Di Giovanni, D. Dobur, A. Drozdetskiy, R.D. Field, M. Fisher, Y. Fu, I.K. Furic, J. Gartner, S. Goldberg, B. Kim, S. Klimenko, J. Konigsberg, A. Korytov, A. Kropivnitskaya, T. Kypreos, K. Matchev, G. Mitselmakher, L. Muniz, Y. Pakhotin, C. Prescott, R. Remington, M. Schmitt, B. Scurlock, P. Sellers, N. Skhirtladze, D. Wang, J. Yelton, M. Zakaria

**Florida International University, Miami, USA**
C. Ceron, V. Gaultney, L. Kramer, L.M. Lebolo, S. Linn, P. Markowitz, G. Martinez, J.L. Rodriguez

**Florida State University, Tallahassee, USA**
T. Adams, A. Askew, D. Bandurin, J. Bochenek, J. Chen, B. Diamond, S.V. Gleyzer, J. Haas, S. Hagopian, V. Hagopian, M. Jenkins, K.F. Johnson, H. Prosper, L. Quertenmont, S. Sekmen, V. Veeraraghavan

**Florida Institute of Technology, Melbourne, USA**
M.M. Baarmand, B. Dorney, S. Guragain, M. Hohlmann, H. Kalakhety, R. Ralich, I. Vodopiyanov

**University of Illinois at Chicago (UIC), Chicago, USA**
M.R. Adams, I.M. Anghel, L. Apanasevich, Y. Bai, V.E. Bazterra, R.R. Betts, J. Callner, R. Cavanaugh, C. Dragoiu, E.J. Garcia-Solis, L. Gauthier, C.E. Gerber, D.J. Hofman, S. Khalatyan, F. Lacroix, M. Malek, C. O'Brien, C. Silvestre, A. Smoron, D. Strom, N. Varelas

**The University of Iowa, Iowa City, USA**
U. Akgun, E.A. Albayrak, B. Bilki, K. Cankocak[43], W. Clarida, F. Duru, C.K. Lae, E. McCliment, J.-P. Merlo, H. Mermerkaya, A. Mestvirishvili, A. Moeller, J. Nachtman, C.R. Newsom, E. Norbeck, J. Olson, Y. Onel, F. Ozok, S. Sen, J. Wetzel, T. Yetkin, K. Yi

**Johns Hopkins University, Baltimore, USA**
B.A. Barnett, B. Blumenfeld, A. Bonato, C. Eskew, D. Fehling, G. Giurgiu, A.V. Gritsan, Z.J. Guo, G. Hu, P. Maksimovic, S. Rappoccio, M. Swartz, N.V. Tran, A. Whitbeck

**The University of Kansas, Lawrence, USA**
P. Baringer, A. Bean, G. Benelli, O. Grachov, M. Murray, D. Noonan, V. Radicci, S. Sanders, J.S. Wood, V. Zhukova

**Kansas State University, Manhattan, USA**
T. Bolton, I. Chakaberia, A. Ivanov, M. Makouski, Y. Maravin, S. Shrestha, I. Svintradze, Z. Wan

**Lawrence Livermore National Laboratory, Livermore, USA**
J. Gronberg, D. Lange, D. Wright

**University of Maryland, College Park, USA**
A. Baden, M. Boutemeur, S.C. Eno, D. Ferencek, J.A. Gomez, N.J. Hadley, R.G. Kellogg, M. Kirn, Y. Lu, A.C. Mignerey, K. Rossato, P. Rumerio, F. Santanastasio, A. Skuja, J. Temple, M.B. Tonjes, S.C. Tonwar, E. Twedt

**Massachusetts Institute of Technology, Cambridge, USA**
B. Alver, G. Bauer, J. Bendavid, W. Busza, E. Butz, I.A. Cali, M. Chan, V. Dutta, P. Everaerts, G. Gomez Ceballos, M. Goncharov, K.A. Hahn, P. Harris, Y. Kim, M. Klute, Y.-J. Lee, W. Li, C. Loizides, P.D. Luckey, T. Ma, S. Nahn, C. Paus, D. Ralph, C. Roland, G. Roland, M. Rudolph, G.S.F. Stephans, K. Sumorok, K. Sung, E.A. Wenger, S. Xie, M. Yang, Y. Yilmaz, A.S. Yoon, M. Zanetti

**University of Minnesota, Minneapolis, USA**
P. Cole, S.I. Cooper, P. Cushman, B. Dahmes, A. De Benedetti, P.R. Dudero, G. Franzoni, J. Haupt, K. Klapoetke, Y. Kubota, J. Mans, V. Rekovic, R. Rusack, M. Sasseville, A. Singovsky

**University of Mississippi, University, USA**
L.M. Cremaldi, R. Godang, R. Kroeger, L. Perera, R. Rahmat, D.A. Sanders, D. Summers

**University of Nebraska-Lincoln, Lincoln, USA**
K. Bloom, S. Bose, J. Butt, D.R. Claes, A. Dominguez, M. Eads, J. Keller, T. Kelly, I. Kravchenko, J. Lazo-Flores, C. Lundstedt, H. Malbouisson, S. Malik, G.R. Snow

**State University of New York at Buffalo, Buffalo, USA**
U. Baur, A. Godshalk, I. Iashvili, S. Jain, A. Kharchilava, A. Kumar, S.P. Shipkowski, K. Smith

**Northeastern University, Boston, USA**
G. Alverson, E. Barberis, D. Baumgartel, O. Boeriu, M. Chasco, S. Reucroft, J. Swain, D. Wood, J. Zhang

**Northwestern University, Evanston, USA**
A. Anastassov, A. Kubik, N. Odell, R.A. Ofierzynski, B. Pollack, A. Pozdnyakov, M. Schmitt, S. Stoynev, M. Velasco, S. Won

**University of Notre Dame, Notre Dame, USA**
L. Antonelli, D. Berry, M. Hildreth, C. Jessop, D.J. Karmgard, J. Kolb, T. Kolberg, K. Lannon, W. Luo, S. Lynch, N. Marinelli, D.M. Morse, T. Pearson, R. Ruchti, J. Slaunwhite, N. Valls, J. Warchol, M. Wayne, J. Ziegler

**The Ohio State University, Columbus, USA**
B. Bylsma, L.S. Durkin, J. Gu, C. Hill, P. Killewald, K. Kotov, T.Y. Ling, M. Rodenburg, G. Williams

**Princeton University, Princeton, USA**
N. Adam, E. Berry, P. Elmer, D. Gerbaudo, V. Halyo, P. Hebda, A. Hunt, J. Jones, E. Laird, D. Lopes Pegna, D. Marlow, T. Medvedeva, M. Mooney, J. Olsen, P. Piroué, X. Quan, H. Saka, D. Stickland, C. Tully, J.S. Werner, A. Zuranski

**University of Puerto Rico, Mayaguez, USA**
J.G. Acosta, X.T. Huang, A. Lopez, H. Mendez, S. Oliveros, J.E. Ramirez Vargas, A. Zatserklyaniy

**Purdue University, West Lafayette, USA**
E. Alagoz, V.E. Barnes, G. Bolla, L. Borrello, D. Bortoletto, A. Everett, A.F. Garfinkel, Z. Gecse, L. Gutay, Z. Hu, M. Jones, O. Koybasi, M. Kress, A.T. Laasanen, N. Leonardo, C. Liu, V. Maroussov, P. Merkel, D.H. Miller, N. Neumeister, I. Shipsey, D. Silvers, A. Svyatkovskiy, H.D. Yoo, J. Zablocki, Y. Zheng

**Purdue University Calumet, Hammond, USA**
P. Jindal, N. Parashar

**Rice University, Houston, USA**
C. Boulahouache, V. Cuplov, K.M. Ecklund, F.J.M. Geurts, J.H. Liu, B.P. Padley, R. Redjimi, J. Roberts, J. Zabel

**University of Rochester, Rochester, USA**
B. Betchart, A. Bodek, Y.S. Chung, R. Covarelli, P. de Barbaro, R. Demina, Y. Eshaq, H. Flacher, A. Garcia-Bellido, P. Goldenzweig, Y. Gotra, J. Han, A. Harel, D.C. Miner, D. Orbaker, G. Petrillo, D. Vishnevskiy, M. Zielinski

**The Rockefeller University, New York, USA**
A. Bhatti, R. Ciesielski, L. Demortier, K. Goulianos, G. Lungu, C. Mesropian, M. Yan

**Rutgers, the State University of New Jersey, Piscataway, USA**
O. Atramentov, A. Barker, D. Duggan, Y. Gershtein, R. Gray, E. Halkiadakis, D. Hidas, D. Hits, A. Lath, S. Panwalkar, R. Patel, A. Richards, K. Rose, S. Schnetzer, S. Somalwar, R. Stone, S. Thomas

**University of Tennessee, Knoxville, USA**
G. Cerizza, M. Hollingsworth, S. Spanier, Z.C. Yang, A. York

**Texas A&M University, College Station, USA**
J. Asaadi, R. Eusebi, J. Gilmore, A. Gurrola, T. Kamon, V. Khotilovich, R. Montalvo, C.N. Nguyen, I. Osipenkov, J. Pivarski, A. Safonov, S. Sengupta, A. Tatarinov, D. Toback, M. Weinberger

**Texas Tech University, Lubbock, USA**
N. Akchurin, J. Damgov, C. Jeong, K. Kovitanggoon, S.W. Lee, Y. Roh, A. Sill, I. Volobouev, R. Wigmans, E. Yazgan

**Vanderbilt University, Nashville, USA**
E. Appelt, E. Brownson, D. Engh, C. Florez, W. Gabella, W. Johns, P. Kurt, C. Maguire, A. Melo, P. Sheldon, S. Tuo, J. Velkovska

**University of Virginia, Charlottesville, USA**
M.W. Arenton, M. Balazs, S. Boutle, M. Buehler, S. Conetti, B. Cox, B. Francis, R. Hirosky, A. Ledovskoy, C. Lin, C. Neu, R. Yohay

**Wayne State University, Detroit, USA**
S. Gollapinni, R. Harr, P.E. Karchin, P. Lamichhane, M. Mattson, C. Milstène, A. Sakharov

**University of Wisconsin, Madison, USA**
M. Anderson, M. Bachtis, J.N. Bellinger, D. Carlsmith, S. Dasu, J. Efron, L. Gray, K.S. Grogg, M. Grothe, R. Hall-Wilton[1], M. Herndon, P. Klabbers, J. Klukas, A. Lanaro, C. Lazaridis, J. Leonard, R. Loveless, A. Mohapatra, D. Reeder, I. Ross, A. Savin, W.H. Smith, J. Swanson, M. Weinberg

†: Deceased
1: Also at CERN, European Organization for Nuclear Research, Geneva, Switzerland
2: Also at Universidade Federal do ABC, Santo Andre, Brazil
3: Also at Laboratoire Leprince-Ringuet, Ecole Polytechnique, IN2P3-CNRS, Palaiseau, France
4: Also at Suez Canal University, Suez, Egypt
5: Also at Fayoum University, El-Fayoum, Egypt
6: Also at Soltan Institute for Nuclear Studies, Warsaw, Poland
7: Also at Massachusetts Institute of Technology, Cambridge, USA
8: Also at Université de Haute-Alsace, Mulhouse, France

9: Also at Brandenburg University of Technology, Cottbus, Germany
10: Also at Moscow State University, Moscow, Russia
11: Also at Institute of Nuclear Research ATOMKI, Debrecen, Hungary
12: Also at Eötvös Loránd University, Budapest, Hungary
13: Also at Tata Institute of Fundamental Research - HECR, Mumbai, India
14: Also at University of Visva-Bharati, Santiniketan, India
15: Also at Facoltà Ingegneria Università di Roma "La Sapienza", Roma, Italy
16: Also at Università della Basilicata, Potenza, Italy
17: Also at Laboratori Nazionali di Legnaro dell' INFN, Legnaro, Italy
18: Also at Università degli studi di Siena, Siena, Italy
19: Also at California Institute of Technology, Pasadena, USA
20: Also at Faculty of Physics of University of Belgrade, Belgrade, Serbia
21: Also at University of California, Los Angeles, Los Angeles, USA
22: Also at University of Florida, Gainesville, USA
23: Also at Université de Genève, Geneva, Switzerland
24: Also at Scuola Normale e Sezione dell' INFN, Pisa, Italy
25: Also at INFN Sezione di Roma; Università di Roma "La Sapienza", Roma, Italy
26: Also at University of Athens, Athens, Greece
27: Also at The University of Kansas, Lawrence, USA
28: Also at Institute for Theoretical and Experimental Physics, Moscow, Russia
29: Also at Paul Scherrer Institut, Villigen, Switzerland
30: Also at University of Belgrade, Faculty of Physics and Vinca Institute of Nuclear Sciences, Belgrade, Serbia
31: Also at Gaziosmanpasa University, Tokat, Turkey
32: Also at Adiyaman University, Adiyaman, Turkey
33: Also at Mersin University, Mersin, Turkey
34: Also at Izmir Institute of Technology, Izmir, Turkey
35: Also at Kafkas University, Kars, Turkey
36: Also at Suleyman Demirel University, Isparta, Turkey
37: Also at Ege University, Izmir, Turkey
38: Also at Rutherford Appleton Laboratory, Didcot, United Kingdom
39: Also at School of Physics and Astronomy, University of Southampton, Southampton, United Kingdom
40: Also at INFN Sezione di Perugia; Università di Perugia, Perugia, Italy
41: Also at Institute for Nuclear Research, Moscow, Russia
42: Also at Horia Hulubei National Institute of Physics and Nuclear Engineering (IFIN-HH), Bucharest, Romania
43: Also at Istanbul Technical University, Istanbul, Turkey